SHEAR STRENGTH OF CIRCULAR REINFORCED CONCRETE COLUMNS

A Thesis

Presented in Partial Fulfillment of the Requirement for

the Degree Bachelor of Science with Distinction in the

College of Engineering of The Ohio State University

By

Lisa Y. Choe

* * * * *

The Ohio State University

2006

Honors Examination Committee:

Dr. Halil Sezen, Advisor

Dr. Rabi Mishalani

Approved by

Advisor
Department of Civil and
Environment Engineering
and Geodetic Science

ABSTRACT

In this research, the influence of parameters on the shear strength of circular reinforced concrete columns is investigated based on the evaluation of experimental data from numerous column tests. Key parameters investigated in shear strength model are the column aspect ratio, axial load, amount of transverse reinforcement, and deformation ductility demand. An examination of existing design equations reveals wide difference in predicted response. Also, the shear strength model for rectangular reinforced concrete columns proposed by Sezen et al. (2004) is used for evaluating whether it is applicable to predict the shear strength of circular columns. The proposed shear strength equation by Sezen et al. (2004) is composed of additive contributions from concrete and transverse reinforcement, and is a function of displacement ductility. The model proposed by Sezen et al. (2004) is compared with contemporary code provisions and previously proposed models using the available column test data and is shown to result in improved accuracy.

This is dedicated to my family.

ACKNOWLEDGMENTS

I would like to thank Dr. Halil Sezen, my advisor, for giving me this incredible opportunity to explore the world of research. Also, I would like to thank Dr. Rabi Mishalani to give me any helpful comments to complete this thesis.

TABLE OF CONTENTS

LIST OF FIGURES AND TABLES

Figures **Page**

Table

Appendix A. Test Column Dimensions and Setup

Figure **Page**

Tables

Appendix B. Force-Displacement Histories

Figure Page

CHAPTER 1

INTRODUCTION

The purpose of this research is to probe the shear strength of circular reinforced columns based on the examination of primary parameters such as the column aspect ratio, axial load, amount of transverse reinforcement, and deformation ductility demand. Also, a shear strength model proposed by Sezen et al. (2004) for use in design and assessment is evaluated based on statistical evaluation of computed and actual shear strength.

It is known that most current designs of reinforced concrete columns to resist earthquakes involve controlling the damage to acceptable levels at a reasonable cost. The structures could survive under seismic attack with little or no apparent damage. When the level of inelastic deformation required is sufficiently low, inelastic strain of the column is such that damage is insignificant. However, some existing reinforced concrete columns built prior to the mid-1970s in high seismic regions are susceptible to seismic attack that would result in massive property damage or collapse (Sezen et al. 2004). Shear failure of reinforced concrete columns can cause to reduce the lateral strength of the building and involve rapid strength degradation. Therefore, it is necessary to evaluate previously proposed models to estimate the shear strength of those older existing columns. Of particular interest in this research is to examine the shear strength calculated by Sezen's

approach (2004) under cyclic loading of circular columns with light and inadequately detailed transverse reinforcement.

1.1 OBJECTIVES AND SCOPE

The first objective of this research is to assess the shear behavior of circular columns exposed to shear failure. This effort is accomplished by evaluating parameters affecting shear strength with data from previous column tests. The second objective is to evaluate previously proposed models that incorporate the following four parameters:

- The first parameter is the column aspect ratio (a/d) defined by the ratio of the shear span, a, to the effective depth, d, as shown in Fig. 1. For cantilever columns, shear span (a) is equal to the length of column; whereas the shear span is equal to a half of column length of columns fixed both ends.

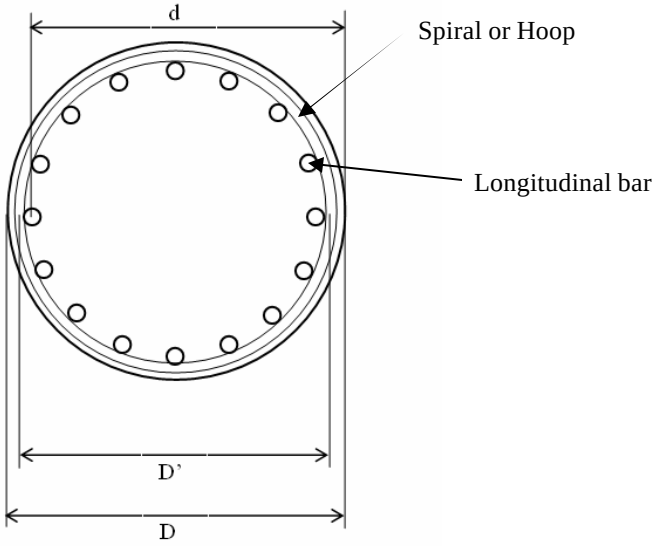

Fig. 1 Definition D, D', and d for the circular column

- The second parameter is the axial load ratio ($P / A_g f'_c$) where P is applied axial load, A_g is a gross cross-sectional area of the circular column, and f'_c is the compressive concrete strength established from compression tests on 28-days moist-cured cylindrical specimens of 6-in. diameter and 12-in. height.
- The third parameter is transverse reinforcement index ($r_w f_y / \sqrt{f'_c}$). r_w is the transverse reinforcement ratio defined by $A_v/(bs)$ where A_v is the area of transverse reinforcement within the hoop or spiral spacing, s, taken as $A_v = 2 A_{sh}$ where A_{sh} is the cross-sectional area of hoops or spirals; b is the width of the column section, equivalent to D for the circular column; and f_y is the yield stress of transverse reinforcement, which depends on the grade of steel.
- The forth parameter considered in this study is deformation ductility demand (m_d) defined by Δ_m / Δ_y where Δ_y is the displacement where the longitudinal steel yields at first, and Δ_m is the maximum displacement under lateral force-displacement histories. The detail mechanism and description of deformation ductility demand are discussed in Section 3.4.

The third objective is to evaluate that the shear model proposed by Sezen et al. (2004) incorporates above parameters. However, it should be noted that this research is narrowed to evaluate the circular columns with aspect ratio larger than 2 with axial load near or below the balanced point, such that those columns are more likely exposed to diagonal tension failure. Consequently, the overall objective of the research is to evaluate whether the shear model proposed by Sezen et al. (2004) can be more practically applied to circular columns having similar configurations and loadings than available models.

1.2 COLUMN CONFIGURATION

Prior to 1970, there was a lack of appreciation regarding the reserve capacity and behavior of structural members approaching shear failure. In the seismically active west coast of the United States, many circular reinforced concrete columns were designed with transverse reinforcement consisting of No. 3 (9.5 mm diameter) or No. 4 (12 mm diameter) spliced hoop reinforcing bars spaced 305 mm (12 in.) on centers, regardless of the cross-sectional area of the column. Consequently, typical transverse reinforcement ratios (r_w) ranged from 0.05% to 0.12% (Priestley et al. 1996).

Fig. 2 shows the typical shear failure of the circular columns built prior to 1970 following California's San Fernando earthquake in 1971. One of primary reasons for column shear failure in the San Fernando earthquake of 1971 and other recent earthquakes were related to poor confinement (Priestley et al. 1996).

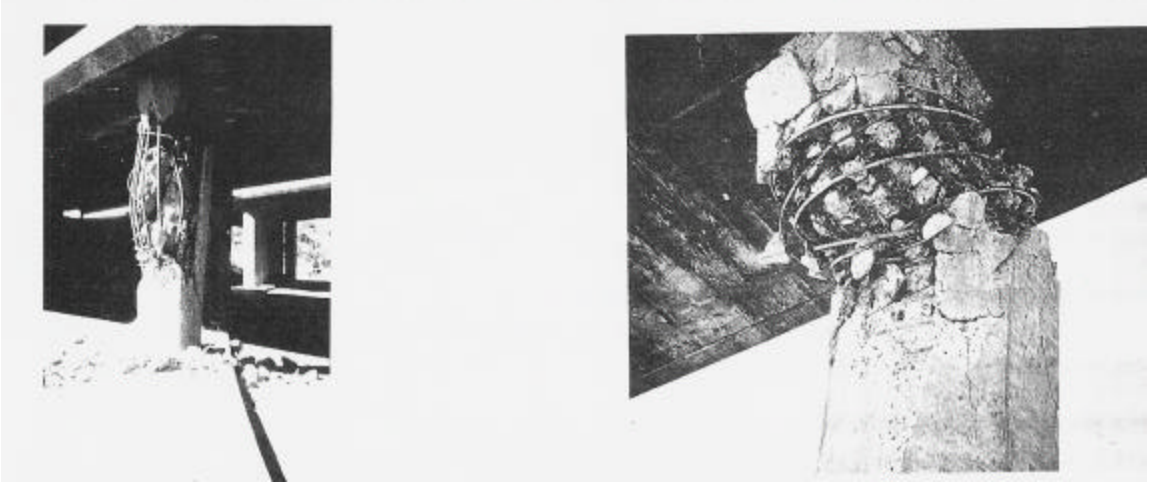

Fig. 2 Typical Shear failure of circular columns, 1971 San Fernando earthquake (Priestley et al. 1996)

Following the San Fernando earthquake, designers have concerned with the behavior of structural components to ensure the actual shear strength of the columns (Priestley et al. 1996). So, most common approach to analyze the shear strength of concrete column sections is a combination of mechanism involving concrete compression shear and truss mechanism utilizing horizontal ties provided by transverse reinforcement (Ghee et al. 1989). However, since columns of older existing reinforced concrete structures were not designed with above shear mechanism, it is necessary to evaluate whether previously proposed models can be applied to the details that are prevalent in those buildings or bridges. Prior to evaluating previously proposed model, it also requires investigating key parameters that characterize the shear strength of circular concrete columns with poorly detailed transverse reinforcement.

1.3 METHODOLOGY

The research described in this study is initiated to examine the important characteristic details of columns observed in existing older structures built prior to mid-1970s. Existing analytical and experimental research on columns of this type is reviewed as the first step. Especially, this research is based on parameters that characterize shear strength of circular test columns such as column aspect ratio, transverse reinforcement index, axial load ratio, and displacement ductility. The second step of this research is to study theoretical and analytical models in terms of literature review on current design codes and previously proposed models. The third step is to evaluate the shear strength models for circular columns with contributions of concrete and transverse reinforcement. Finally, by applying previously proposed models to compute shear strength of test

columns, statistical evaluation of computed and actual shear strengths obtained from laboratory tests can be examined. In this project, the following steps are followed:

- The configuration of circular reinforced column and parameters that affect shear strength of reinforce concrete columns reported in literature are discussed. Shear strengths of circular columns are evaluated by exploring and modifying the model reported in the primary reference: "Shear Strength Model for Lightly Reinforced Concrete Columns" by Halil Sezen and Jack P. Moehle, Journal of Structural Engineering (2004). Also, existing shear strength models including ACI 318-2005 (2005), Standard New Zealand (1995), ASCE-ACI 426 approach, Caltrans, ATC-32, and Priestley's approach (1994) are described as a part of literature review.
- The test results of fifty specimens are selected, which are available in column database compiled by the researchers at the University of Washington (www.ce.washingtong.edu/~peera1/) and by the Kawashima research group at the Tokyo Institute of Technology (www. seismic.cv.titech.ac.jp/en/).
- The columns included in this research satisfy the following criteria: column aspect ratio, $2 \le a/d \le 4$; concrete compressive strength, $13 \le f'_c \le 45$ MPa; longitudinal and transverse reinforcement nominal yield stress depending on the grade of reinforcing steels, f_{yl} and f_y in the range of 300 - 650 MPa; longitudinal reinforcement ratio defined by the ratio of longitudinal steel area to the gross cross-sectional area of a column , $0.01 \le r_l \le 0.04$; transverse reinforcement index, $0.01 f'_c \le r_w f_y \le 0.12 f'_c$; and columns were either fixed at both ends or cantilever.

- Excel spreadsheets are used as a primary tool for the examination of experimental data in order to evaluate the configuration of columns and key parameters. Based on statistical evaluation of data with the primary parameters and theoretical formulations, previously proposed models are evaluated to predict the shear strength of the circular column.

CHAPTER 2

LITERATURE REVIEW

2.1 CONTEMPORARY CODE PROVISIONS AND PROPOSED MODELS FOR SHEAR STRENGTH OF CIRCULAR REINFORCED CONCRETE COLUMNS

The following section provides a review of the shear strength provisions of various contemporary design code and proposed models. Most design codes include contributions from concrete and transverse reinforcement to analyze the shear strength of circular columns. The two components are then summed to estimate the total shear strength.

ACI 318-2005 (2005)

The current ACI code [ACI 318-2005] considers a portion of the design shear force to be carried by the concrete shear resisting mechanism, V_c, with the remainder carried by truss mechanism, V_s, involving transverse reinforcement.

$$V_n = V_c + V_s \tag{1}$$

The ACI code presents the following equation for calculating V_c for members subjected to combined shear, moment, and axial compression:

$$V_c = 0.166\left(1+\frac{P}{13.8A_g}\right)\sqrt{f_c'}bd \quad \text{(Units: MPa)} \tag{2}$$

where P is axial load subjected to the column; A_g is gross cross-sectional area of the column; f'_c is concrete compressive strength; and b is the width of column; and d is the effective depth of column. The transverse reinforcement contribution is also calculated as

$$V_s = \frac{A_v f_y d}{s} \tag{3}$$

where A_v is the area of transverse reinforcement within the spacing, s, and f_y is the yield stress of hoops or spirals.

Standard New Zealand (1995)

Standard New Zealand (1995) adapted the following equations based on a 45-degree truss model for the nominal shear strength of concrete columns. In determination of V_c inside the plastic hinge zone, the longitudinal steel amount and the axial load effect are considered. However, the axial load effect is applied only if the axial load ratio exceeds 0.1. If the axial load ratio is less than or equal to 0.1, the concrete contribution to shear strength is ignored. The shear strength carried by concrete is thus calculated as

$$V_c = \left(4(0.07+10r_w)\sqrt{f'_c}\sqrt{\frac{P}{f'_c A_g}-0.1}\right)bd \quad \text{(Units: MPa)} \tag{4}$$

where the transverse reinforcement ratio, r_w is calculated as

$$r_w = \frac{A_v}{bs} \tag{5}$$

where A_v is the area of transverse reinforcement within spacing, *s*, and *b* is the width of the column. For circular columns, *b* is taken as the column diameter, *D*.

The shear strength carried by transverse reinforcement is based on analysis of effective shear resistance provided by transverse hoops assuming a 45-degree truss mechanism (Ghee et al. 1989). V_s is thus calculated as

$$V_s = \frac{p}{2}\frac{A_{sp} f_{yh} D_{sp}}{s} \tag{6}$$

where A_{sp} is the cross-sectional area of spirals or hoops, D_{sp} is the core diameter of circular column defined by the center-to-center diameter of hoops or spirals; f_{yh} is yield stress of transverse steel; and *s* is vertical distance between transverse hoops or spirals.

ASCE-ACI 426 Shear strength Approach

Committee 426, a joint ASCE-ACI committee on shear strength of concrete members, has produced design equation based on the additive model given in Eq. (1). They do not consider the influence of ductility to estimate total shear strength of circular columns (Priestley et al. 1994).

The shear strength carried by concrete, V_c, is calculated by Eq. (7)

$$V_c = v_b\left(1+\frac{3P}{f'_c\,A_g}\right)A_e \tag{7}$$

where A_e is the effective shear area of circular column with diameter D, taken as Eq. (8), and v_b is the nominal shear stress carried by concrete, calculated by Eq. (9);

$$A_e=0.8A_{gross}=0.628D^2 \tag{8}$$

where D is diameter of circular column

$$v_b=(0.066+10\,r_t)\sqrt{f'_c}\le 0.2\sqrt{f'_c} \quad \text{(Units:MPa)} \tag{9}$$

where r_t is the longitudinal tension steel ratio, taken as 0.5 r_l for columns (Priestley et al. 1994). r_l is estimated by the ratio of longitudinal steel area within the column section to gross cross-sectional area of columns. It is also assumed that transverse reinforcement contributes to stabilizing diagonal compression struts at $q=45^o$ to the member axis to produce the strength, V_s:

$$V_s=\frac{p}{2}\frac{A_h f_{yh} D'}{s} \tag{10}$$

where D' is the diameter of the spiral or hoop.

ATC-32 Shear Design Equations

Design approach of ATC-32 Report (1996) also uses the combination of concrete shear resisting mechanism, V_c, and steel shear resisting truss mechanism, V_s. Nominal

shear strength V_n and V_s are given by Eq. (1) and Eq. (10), respectively. The formula for V_c is the following:

$$V_c = 0.167\left(k_1 + \frac{P}{k_2 A_g}\right)\sqrt{f'_c}(0.8A_g) \quad \text{(Units:MPa)} \tag{11}$$

In Eq. (11), k_1 = 1.0, except in plastic hinge regions of ductile columns, where k_1 = 0.5, and k_2 = 13.8 for compressive axial load P and k_2 = 3.45 for tensile axial load where P has the negative sign.

CALTRANS MEMO 20-4

The Caltrans shear strength equations are primarily intended as an assessment tool for determining the shear strength of existing bridge columns (Kowalsky et al. 2000). This approach recognizes the effect of displacement ductility on column shear strength, and nominal shear strength is based on the following equations for V_c and V_s. The transverse reinforcement shear capacity estimated by Caltrans is given by Eq. (6), and shear carried by concrete is calculated by Eq. (12).

$$V_c = v_c A_e = F_1 F_2 \sqrt{f'_c}(0.8A_g) \le 0.33\sqrt{f'_c}A_g \quad \text{(Units:MPa)} \tag{12}$$

In Eq. (12) the normalized shear stress of concrete, v_c, is a function of the product of F_1 and F_2, which are the terms related to the shear strength dependent on displacement ductility level, m_d, and axial load ratio, P/A_g. Displacement ductility level is estimated by the ratio of measured maximum displacement (Δ_m) to measured yield displacement (Δ_y)

under cyclic loading, and the detailed descriptions are available in Section 3.4. So, the factors F_1 and F_2 can be numerically calculated by Eq. (13), (14), and (15).

$$F_1 = 0.025 \le 0.08 r_w f_{yh} + 0.305 - 0.083 m_d \le 0.25 \quad (13)$$

where r_w is transverse reinforcement ratio, and f_{yh} is the yield stress of hoops or spirals.

$$F_2 = 0 \text{ for } P/A_g < 0 \quad (14)$$

$$F_2 = \left(1 + \frac{P}{13.8 A_g}\right) \le 1.5 \text{ for } P/A_g = 0 \quad (15)$$

where P is axial load subjected to the column, and A_g is the gross cross sectional area.

Approach of Priestley et al. (1994)

Priestley et al. (1994) indicates that the ASCE-ACI 426 approach for shear strength does not provide good estimate of the shear strength of columns. For low ductility levels, the approach tends to be excessively conservative, while at high ductility levels it is in some cases non-conservative. Priestley et al. (1994), therefore, proposes a model for the shear strength of columns under cyclic lateral load as the summation of strength contribution from concrete, V_c, a truss mechanism, V_s, and an arch mechanism associated with axial load, V_p.

$$V_n = V_c + V_s + V_p \quad (16)$$

where $V_c = k\sqrt{f'_c}\, A_e$, $A_e = 0.8 A_{gross}$

Also, k within plastic end regions depends on the member of displacement ductility m_d as defined in Fig. 3

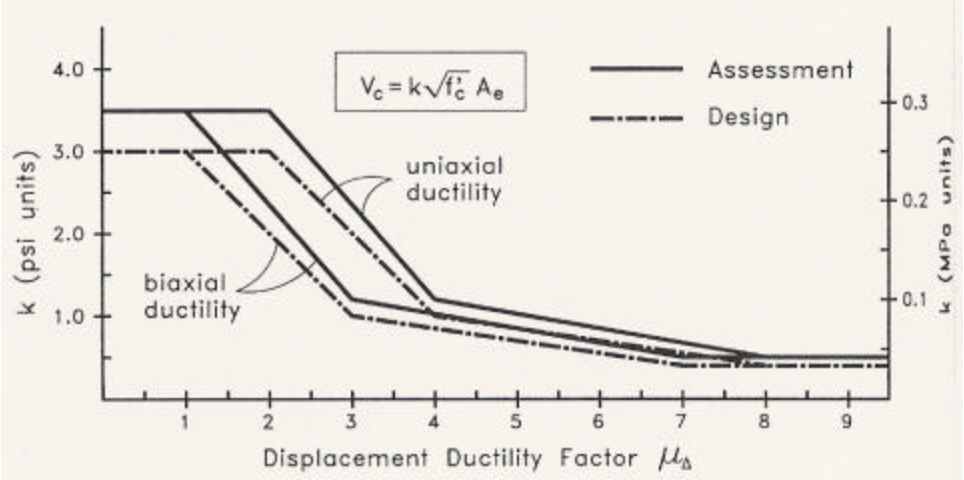

Fig. 3 Relationship between ductility and strength of concrete shear-resisting (Seismic Design and Retrofit of Bridges by Priestley et al. 1996)

The truss mechanism strength for circular columns is given by

$$V_s = \frac{p}{2}\frac{A_h f_{yh} D'}{s}\cot q \tag{17}$$

The angle of the critical inclined flexure-shear cracks to the column axis is taken as $q = 30^o$, unless limited to larger angles by the potential corner-to-corner crack. The shear strength enhancement resulting from axial compression is considered as a variable, and is given by

$$V_p = P\tan a \;=\; \frac{D-c}{2a}P \tag{18}$$

where *D* is the diameter of circular column; *c* is the depth of the compression zone; and shear span, *a*, is *L* for a cantilever column. For a cantilever column, *a* is the angle formed between the column axis and the strut from the point of load application to the center of the flexural compression zone at the column plastic hinge critical section. As shown in Fig. 4, for a column in double bending, a is the angle between the column axis and the line joining the centers of flexural compression at the top and bottom of the column.

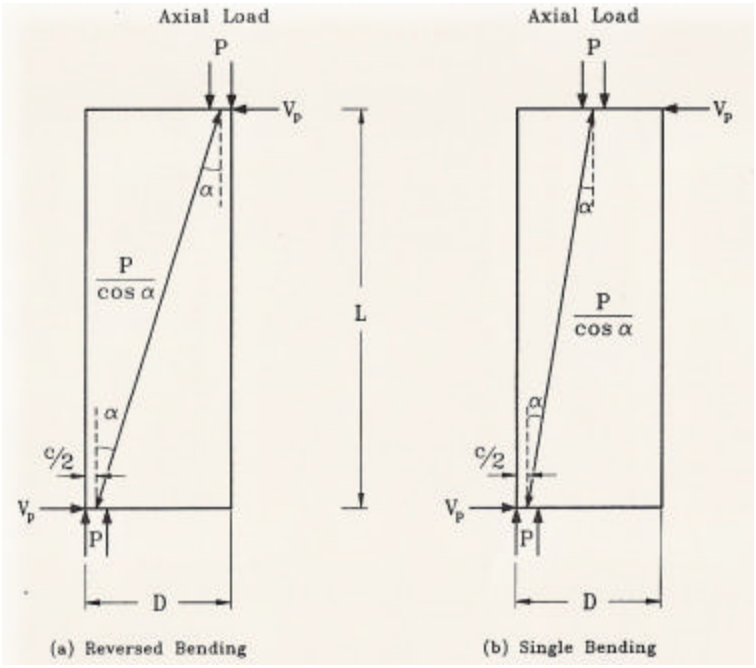

Fig. 4 Contribution of axial force to column shear strength (Seismic Design and Retrofit of Bridges by Priestley et al. 1996)

2.2 TEST CONFIGURATIONS OF PREVIOUS RESEARCH AND EXPERIMENTAL DATA

This section provides a review of previous experimental researches on the shear behavior and deformation characteristics of circular reinforced concrete columns. The results from cited experimental studies are intended to be applicable to circular columns under lateral loading where strength is governed by either by shear or by flexure followed by shear failure. This research on shear strength model of circular column is focused on the data analysis available from previous tests; therefore, it is helpful to review for defining test geometries and load histories that are investigated in the present study. Column geometries and test setups are provided in Appendix.

TESTS TO STUDY SHEAR BEHAVIOR

Ghee et al. (1985) tested twenty five circular columns under constant axial loads and cyclic lateral displacements. The experimental program was divided into two stages. In the first stage, 25 cantilever circular columns were subjected to slow cyclic loading with gradually increasing displacement limits to simulate earthquake loadings. Fig. A.1 in Appendix shows details and overall dimensions of column specimens. In the second stage of the project, the conclusion drawn from these experimental tests were then examined by dynamic tests on a shake-table to simulate how test columns behave under seismic load.

The main parameters employed in experiments were the ratio of height to diameter of column (L/D), where L is the height of column, and D is diameter of the circular column; the axial load level (P/f'_cA_g); and the volumetric spiral reinforcement content

($r_s = 4A_{sp}/(ds)$) where A_{sp} is the cross sectional area of spirals; d is depth of the column; and s is the spacing of hoops or spirals. The main ratios of height to diameter of column (L/D) were 1.5, 2.0, 2.5, and 1.75 (Unit 20). Levels of axial compression (P/f'_cA_g) used were 0, 0.1, and 0.2. The main volumetric spiral reinforcement content varied between 0.0038 and 0.00102.

In addition, under monotonic loading, four major failure modes were identified as follows: 1) ductile flexural (D-F) with the column units that achieved ductility levels grater than 6 without any indication of shear failure; 2) moderately ductile with shear failure (MD-S) when columns failed with the ductility level between 4 and 6; 3) limited ductile with shear failure when the column achieved the ductility of column between 2 and 4; and 4) brittle failure with the column that exhibited shear failure.

Wong et al. (1993) tested sixteen circular cantilever columns having the height to diameter of the column ratio (L/D) of 2 and different spiral reinforcement contents to investigate the sensitivity of the strength and stiffness of shear-resisting mechanisms. Three levels of axial compression load, P = 0, 0.19 $f'_c A_g$, and 0.39 $f'_c A_g$, were applied. The spiral reinforcement content, r_s, varied between 0.39 and 2.46. Column units (Fig. A.2) were attached to a *self-reacting frame* to represent horizontal two-dimensional seismic effect.

Columns also were tested with the application of quasi-static lateral forces under constant axial compression loads. Four types of displacement were used as shown on Fig. A.3. including *uniaxial u-type displacement pattern* with one load cycle consisted of an East-West (E-W) path; *biaxial b-type displacement pattern* with one cycle of a North-

South path followed by an E-W; *biaxial s-type displacement pattern* with a complete cycle, composed of four displacement loops; and *multi-directional r-type displacement pattern* using dynamic time-history analyses. Compared with uniaxial displacement paths, biaxial displacement patterns caused more severe degradation of strength and stiffness. However, the displacement ductility capacity was not sensitive to the biaxial displacement pattern.

Nelson (2000) tested four poorly confined reinforced concrete columns to evaluate the effects of long-duration earthquakes on bridge columns. For the analysis of both force-displacement column response and damage progression, four identical columns are designed with aspect ratio of 3 as shown on Fig. A.4. The geometry of test columns was consistent with a prototype of a Washington State Department of Transportation circular bridge column built prior to mid-1970s. Also, columns were subjected to different lateral-loading histories. Four patterns of damage strongly influenced by the displacement demand were observed: 1) the first yield of the longitudinal reinforcement; 2) significant flexural cracking; 3) significant spalling; and 4) residual cracking. The resulting range of displacement and energy dissipation that resulted in each damage level is shown in Table 1.

Damage Level	Displacement (inches)		Energy Dissipation (kip-inches)	
	Lower Bound	Upper Bound	Lower Bound	Upper Bound
First Yield of Longitudinal Reinforcement	0.35	0.39	12.4	31.2
Bar Buckling (observed)/ Hoop Fracture	1.77	2.23	199	599
Loss of Axial Load Capacity	1.80	3.54	637	930

Table 1. Measured Boundary Values of Damage Level Parameters (Nelson 2000)

Sritharan et al. (1996) tested three circular columns. In all three designs, force transfer models were employed to determine the amount of joint reinforcement as the design parameter. In particular, the cap beam was supported at the ends of the column. Axial compressions in the cap beam acts to improve the joint performance with the opposite applying for the axial tension in the beam. The test set-up and overall dimensions of the test unit are shown in Fig. A.5.

Verma et al. (1993) tested eight columns with the height to diameter of the column ratio (*L/D*) of 2.0 or 1.5, similar to the typical details of a squat circular prototype bridge column designed and constructed prior to 1970s. Fig. A.6 (a) and (b) illustrate the typical reinforcement details of the test columns. A total of eight columns tested under double bending with two separate conditions: four columns were tested in the "as-built" condition and the remaining four as retrofitted columns with full height of cylindrical steel jacket. Axial load level of the test columns was in the range of $0.06 = P / f'_c A_g = 0.18$, corresponding to an axial load (*P*) between 848 kips and 2544 kips, respectively.

An increase in the axial load ratio represented a more severe case as associated with a decrease in the ductility capacity and a much more rapid and brittle strength degradation after shear failure.

Ohtaki et al. (1996) tested the cantilever column L1 under cyclic loading to investigate the shear strength of existing bridge piers and the effectiveness of fiberglass for increasing shear strength after shear failure. The column unit L1 was designed as a pre-1971 ordinary bridge column with the span to depth ratio (*L/D*) of 2.0. No axial force was applied except for the column weight and the weight of actuators, corresponding to an axial force (*P*) of 220 kN. The details of the test unit are shown in Fig. A.7. First flexural cracks were observed at a lateral force of 590 kN, and flexural cracks started to incline at shear force of 1280 kN, corresponding to an average nominal shear stress of $0.11\sqrt{f'_c}$ MPa. The column failed before the first peak of ductility factor μ =1.5, and maximum crack width observed at failure was about 10 mm.

McDaniel (1997) tested three circular concrete columns (S1, S1-2, and S2) which were one-third scale of model of a full scale column, L1 tested by Ohtaki et al. (1996), to investigate the effects of scale on the concrete component of shear strength. The details of test model units are shown in Fig. A.8. The force displacement envelopes for the three tests followed nearly identical paths, with a residual displacement after failure of approximately 6 mm for S1-2 and S2, and scaled value of approximately 6 mm for L1 as well. Each column failed in shear at a displacement ductility of 1.5. The ultimate force level for units S 1-2 and S2 was 332 kN, approximately 1/9 of Unit L1's ultimate force of

3105 kN. Ultimate displacement of S 1-2 and S2 was 8 mm, and approximately 1/4 of Unit L1's ultimate displacement of 33 mm. Unit S1 was modified to have the additional shear contribution provided by the curvature rods, and it failed at 313 kN at a displacement of 10.68 mm.

Benzoni et al. (1996) tested four circular reinforced concrete columns under cyclic inelastic lateral displacements with different axial loads. Four specimens (CS1, CS2, CS3, and CS4) were tested in double bending with the span to depth ratio (*L/D*) of 2. The details of the model test units are shown in Fig. A.9. The test units of CS1 and CS2 were subjected to an axial load ratio of 0.35 and -0.087, considered as typical upper and lower limits of axial load for bridge columns. The other units of CS3 and CS4 were tested under the axial load range between two previous limits, as a function of the applied horizontal load. First flexural cracks of Unit CS1 were observed at a lateral force of 200 kN, and shear inclination of flexural cracks was indicated at 334 kN. For unit CS2, horizontal cracks appeared during complete cycles to a peak horizontal force of 40 kN to 250 kN. The maximum lateral forces were 359 kN in push direction and -284 kN in pull direction at m_d =2.0. The test was finished at m_d =6 without longitudinal or transverse reinforce fracture. For unit CS3, the maximum lateral forces obtained were 509.5 kN in push direction and 306.6 kN in pull direction at m_d =2.0. For unit CS4, major widening of existing cracks were observed at m_d =1.5.

In this chapter, previous researches on shear strength models and experimental studies of circular columns have been discussed. To evaluate the parameters affecting shear

strength of circular columns and previously proposed shear strength models, columns included in cited studies are selected by the criteria discussed in Section 1.3. Table 2 summarizes all the test variables of 50 columns used to estimate shear strengths. Based on column properties in Table 1 and the force-displacement histories in Appendix, next step is to evaluate parameters affecting shear strength and to evaluate existing shear strength models.

		D (mm)	cover (mm)	d_h (mm)	d_l (mm)	a (mm)	s (mm)	$?_l$ (%)	$?_w$ (%)	f_{yl} (Mpa)	f_{yh} (Mpa)	f'_c (Mpa)	P (kN)	m_d	V_{test} (kN)
No.1	Ghee (1985)	400	15	6.0	16	800	60	3.20	0.51	436	328	37.5	0	2.7	321
No.2		400	15	6.0	16	800	60	3.20	0.51	457	328	37.2	0	4.9	221
No.3		400	15	6.0	16	1000	60	3.20	0.51	436	328	36.0	0	3.9	276
No.4		400	15	10.0	16	800	165	3.20	0.51	436	316	30.6	0	1.5	289
No.5		400	15	6.0	16	800	40	3.20	0.76	436	328	31.1	0	2.4	331
No.7		400	15	6.0	16	800	80	3.20	0.38	448	372	29.5	0	1.5	281
No,9		400	15	6.0	16	1000	30	3.20	1.02	448	372	29.9	0	3.2	445
No.10		400	15	12.0	16	800	120	3.20	1.02	448	332	31.2	784	3.6	437
No.11		400	15	6.0	16	800	60	3.20	0.51	448	372	29.9	751	2.6	407
No.13		400	15	6.0	16	800	30	3.20	1.02	436	326	36.2	455	4.0	436
No.14		400	15	6.0	24	800	60	3.24	0.51	424	326	33.7	0	1.9	316
No.15		400	15	6.0	16	800	60	1.92	0.51	436	326	34.8	0	4.5	230
No.16		400	15	6.0	16	800	60	3.20	0.51	436	326	34.4	420	1.3	352
No.17		400	15	6.0	16	1000	60	3.20	0.51	436	326	34.3	431	1.7	312
No.21		400	15	6.0	16	800	80	3.20	0.38	436	326	33.2	0	5.1	271
No.22		400	15	10.0	16	800	220	3.20	0.39	436	310	30.9	0	2.5	285
No.23		400	15	12.0	16	800	160	3.20	0.76	436	332	32.3	0	1.7	333
No.24		400	15	10.0	16	800	110	3.20	0.77	436	310	33.1	0	4.1	341
Col1	Nelson (2000)	508	19	4.5	16	1524	102	0.99	0.13	455	455	56.2	1450	4.1	283
Col3		508	19	4.5	16	1524	102	0.99	0.13	455	455	57.0	1139	3.1	260
Col4		508	19	4.5	16	1524	102	0.99	0.13	455	455	52.7	1139	4.4	252
UCI 3	Hamilton (2002)	406	8.2	4.5	13	1048	171.5	1.37	0.10	459	492	34.5	0	2.7	143
UCI 4		406	8.2	4.5	13	1048	171.5	1.37	0.10	459	492	34.5	0	1.6	164
UCI 5		406	8.2	4.5	13	1048	63.5	1.17	0.26	459	492	35.4	0	5.1	170
*No.1	Wang et al. (1990)	400	15	10.0	16	800	60	3.20	1.42	423	300	38.0	907	7.0	461
No.2		400	15	6.0	16	800	65	3.20	0.47	475	340	37.0	1813	3.9	489
*No.3		400	15	10.0	16	800	60	3.20	1.42	475	300	37.0	1813	6.5	579
M2E1	Petrovsky (1984)	307	33	6.0	12	900	75	1.83	0.63	240	240	35.9	145	3.5	-86
M2E2		307	33	6.0	12	895	75	1.83	0.63	240	240	34.4	254	3.6	-93
NH5	Vu (1998)	457	20	9.5	16	910	80	2.41	0.85	508	448	35.2	-490	3.9	403
IC1	Sritharan (1996)	600	25.4	9.5	22	1800	97	1.92	0.54	448	431	31.4	400	5.7	387
IC2		600	25.4	9.5	22	1800	97	1.92	0.54	448	431	34.6	400	5.8	411
IC3		600	25.4	2.7	7	1500	14.48	1.98	0.68	446	476	25.4	120	3.0	433
verma 1	Verma (1993)	610	13.97	6.4	19	1219	127	2.53	0.17	324	359	31.0	591.9	2.5	129
verma 3		610	13.97	6.4	19	1219	127	2.53	0.17	324	324	34.5	1780	3.0	165
verma 5		610	13.97	6.4	19	1219	127	2.53	0.17	469	324	35.9	591.9	1.0	138
L1	Ohtaki (1997)	1829	50.8	12.7	43	3658	304.8	1.33	0.10	508	298	29.6	355.9	1.8	3104
CS1	Benzoni (1996)	460	15.24	6.4	16	910	95.3	2.50	0.25	462	369	29.3	1690	2.1	493
*CS2		460	15.24	6.4	16	910	95.3	2.50	0.25	462	369	35.8	-512	2.2	322
CS3		460	15.22	6.4	16	910	95.3	2.50	0.25	462	369	37.0	1690	2.5	409
S1	McDaniel (1997)	610	16	4.9	16	1219	101.6	1.36	0.13	454	200	29.8	18.8	3.5	406
S1-2		610	16	4.9	16	1219	101.6	1.36	0.13	454	200	26.8	18.8	1.4	-332
S2		610	16	4.9	16	1219	101.6	1.36	0.13	438	200	31.2	18.8	1.6	-332
*TP 54	Kawashima lab.	400	27	6.0	13	1350	50	2.02	0.75	377	374	22.4	180	6.5	228
*TP 55		400	27	6.0	13	1350	50	2.02	0.75	377	374	22.4	180	5.1	251
*TP 57		400	27	6.0	13	1350	50	2.02	0.75	377	374	22.3	180	2.0	224
*TP 60		400	27	6.0	13	1350	60	2.02	0.75	377	374	27.8	180	4.9	230
*TP 61		400	27	6.0	13	1350	60	2.02	1.49	377	374	27.8	180	6.0	229

* Experimental yield displacement was not reported

Table 2 Dimensions, Material Properties, and Other Details for Specimens Included in the Database

CHAPTER 3

EVALUATION OF PARAMETERS AND PROPOSED SHEAR STRENGTH MODEL

This section discusses parameters to analyze the shear strength of circular columns including column aspect ratio, longitudinal reinforcement, transverse reinforcement, and axial load. Also, existing shear strength models discussed in Section 2.1 are investigated in terms of above parameter in addition to displacement ductility demand. The model proposed by Sezen et al. (2004) is then evaluated by statistical comparison with previous models discussed in Section 2.1 to show the result in improved accuracy.

3.1 EVALUTATION OF PARAMETERS

Sezen et al. (2004) identifies key parameters affecting the shear strength of rectangular columns, which are the column aspect ratio, axial load, amount of transverse reinforcement, and deformation ductility demand. The cited models in this study also consider similar parameters based on statistical evaluation of experimental data from test results. Fig. 5 shows the variation of maximum measured shear strength (V_{test}) under cyclic loading for the columns included in Table 2 as a function of above parameters. For

the evaluation of the circular shear strength of circular columns, the measured shear strength, V_{test}, is normalized by "the product of the square root of the measured concrete compressive strength and the gross cross-sectional area of the column" (Sezen et al. 2004). The following key points are observed.

- Fig. 5 (a) plots normalized shear strength as a function of $P / A_g f'_c$, where P = axial compressive force at time of shear failure; A_g = gross cross-sectional area; and f'_c = measured concrete compressive strength. This plot shows the trend (indicated by the dashed line in the figure) that shear strength increases with increasing axial compression.
- Fig. 5 (b) plots normalized shear strength as a function of longitudinal reinforcement ratio. It shows the trend that shear strength increases with increasing longitudinal reinforcement ratio.
- Fig. 5 (c) plots normalized shear strength as a function of aspect ratio, *a/d*, where *a* = distance from point of maximum moment to point of zero moment, and *d* = distance from extreme compression fiber to centroid of longitudinal tension reinforcement. It shows the trend that shear strength decreases with increasing *a/d*.
- Fig. 5 (d) plots normalized shear strength as function of transverse reinforcement index, $r_w f_y / \sqrt{f'_c}$ where r_w = transverse reinforcement ratio; f_y = yield stress of the transverse reinforcement; and f'_c = concrete compressive stress. It shows the trend that shear strength increases with increasing amount of transverse reinforcement.

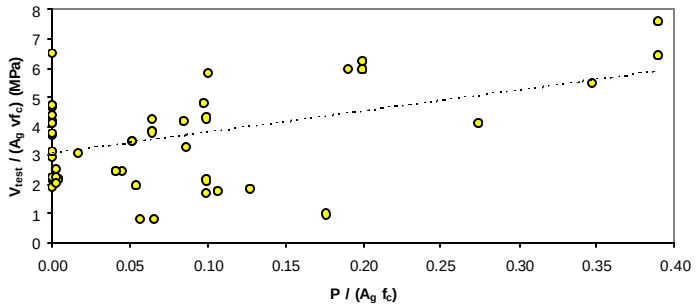

(a)

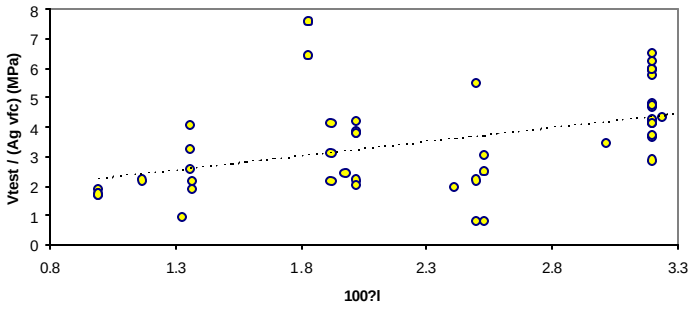

(b)

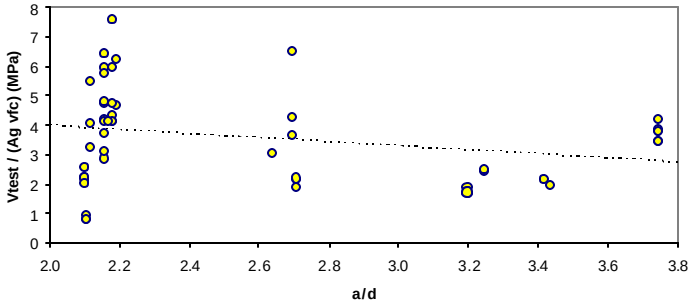

(c)

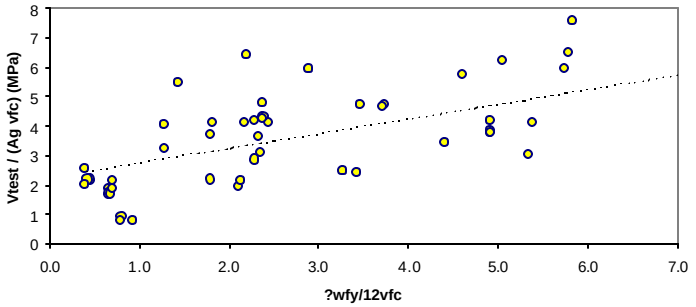

(d)

Fig. 5 Relationship between normalized shear strengths and test parameters including (a) axial load ratio; (b) longitudinal reinforcement ratio; (c) aspect ratio; and (d) transverse reinforcement index

3.2 CONCRETE CONTRIBUTION

In this section, to evaluate shear strength carried by concrete, Sezen's approach (2004) of shear strength carried by concrete is used as the primary reference. The following summarizes the shear mechanism of concrete contribution developed by Sezen et al. (2004) in order to estimate shear strength of rectangular concrete columns.

Shear failure of reinforced concrete columns in older existing buildings and bridges built in prior 1970s are typically observed as either diagonal tension failure or diagonal compression failure. Diagonal compression failure can occur either before or after inclined cracks are formed in concrete columns with low aspect ratio. On the other hand, diagonal tension failure would be the mode of shear failure following the formation of inclined cracks. As loading continues, crack opening becomes larger, such that it may result in failure due to the rapid degradation of the load-carrying mechanism. For the case of columns with aspect ratio (*a/d*) larger than 2 with axial loads near or below the balanced point, diagonal tension failure tends to be a more significant mode of filature in shear. Since in this study test column data are collected with $2 \le a/d \le 4$, the goal can be limited to develop a model to predict the diagonal tension capacity. The major assumption to estimate the maximum shear carried by concrete is that "at onset of diagonal tension cracking, the element under uniform stress is subjected to the nominal principal tension stress" (Sezen et al. 2004). Therefore, the shear carried by concrete at diagonal tension cracking can be defined by the following equation:

$$V_c = \frac{0.5\sqrt{f'_c}}{a/d}\sqrt{1+\frac{P}{0.5\sqrt{f'_c}A_g}}0.8A_g \quad \text{(MPa)} \tag{19}$$

Equation (19) indicates that V_c is increased with axial load ratio and with decreasing aspect ratio, and this result is matching with the relation between shear strength and parameters discussed in Section 3.1.

3.3 TRANSVERSE REINFORCEMENT CONTRIBUTION

It is assumed that transverse reinforcement contributes to stabilizing diagonal compression struts at $q = 45^0$ to the longitudinal axis of the column to produce strength, $V_s = aA_v f_y d / s$ (MacGregor 1997). For circular sections reinforced with spirals or circular hoops, codes have generally recommended taking $A_v = 2\ A_h$ because there are two legs of hoops or spirals across the shear section of the circular column. The value of a has been defined diversely by previous studies and code specifications (MacGregor 1997; Sezen et. al. 2004). To estimate shear carried by transverse reinforcement in this study, it is assumed that shear-resisting force of hoops or spiral is exposed by the presumed 45-degree angle of diagonal tension cracking (Ghee et al. 1989), which is as shown in Fig 6. Another assumption is that spacing, *s*, is sufficiently small compared with the core diameter *D'*. The shear carried by transverse reinforcement, V_s, can be calculated by Eq. (20)

$$V_s = \frac{p}{2}\frac{A_h f_{yh} D'}{s} \tag{20}$$

Above equation indicates that shear capacity contributed by transverse reinforcement is proportional to the amount of transverse reinforcement. This result agrees with the

correlation between shear strength and transverse reinforcement index discussed in Section 3.1

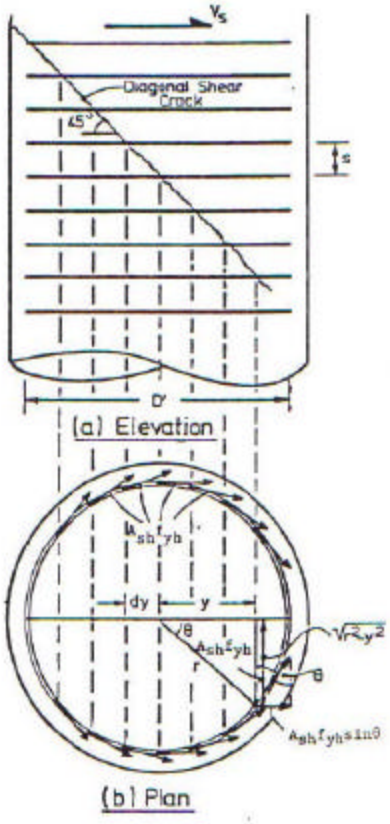

Fig. 6 Shear Carried by Transverse Reinforcement for Circular Column (Ghee et. al 1989)

3.4 SHEAR STRENGTH-DUCTILITY RELATIONSHIP

The effect of displacement ductility demand on seismic shear strength has generated controversy among many researchers because shear failures of reinforced concrete column occur extensively (Priestly et al. 1996). The relation between shear strength and displacement ductility demand can be examined using the column test data in Table 2.

Fig. 7 plots the ratio of measured (V_{test}) to calculated shear strength (V_n) as a function of displacement ductility. Measured shear strengths are referred to Table 2, and calculated shear strengths for 50 columns included in this study are obtained by Eq. (1), (19), and (20). The dashed line in Fig. 7 indicates the trend that the ratio of measured to calculated shear strength decreases with increasing displacement ductility.

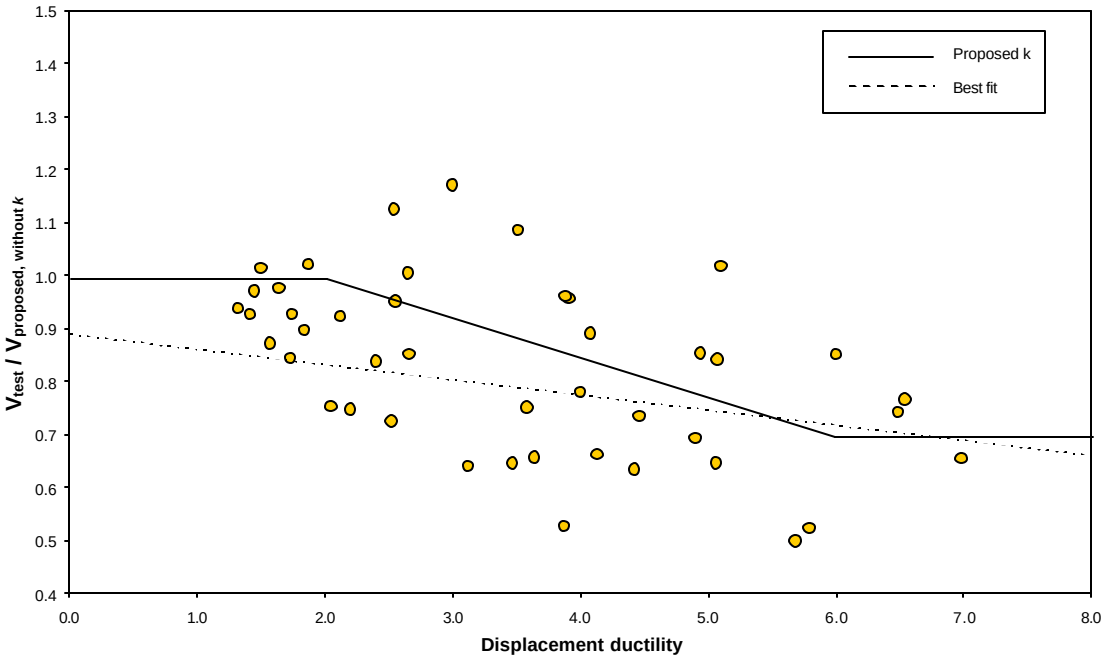

Fig. 7 Shear strength degradation with displacement ductility

For seismic design of reinforced concrete columns, it has been assumed that satisfactory response of a circular column under earthquake attack depends on the capacity of the column to displace inelastically through several cycles of loading without significant degradation of strength or stiffness, a quality termed *ductility* (Priestly et al. 1996). As shown in displacement relationship of Fig. 8, yield displacement (Δ_y) is the

first measured displacement where deformation continues without increasing lateral load. Maximum displacement (Δ_m) is the displacement at base shear force (V_d) about 80 % of maximum applied shear stress (V_{test}) (Sezen et al. 2004). If the maximum displacement expected during the design-level earthquake is Δ_m, the maximum expected displacement ductility factor is defined as

$$m_d = \frac{\Delta_u}{\Delta_y} \tag{21}$$

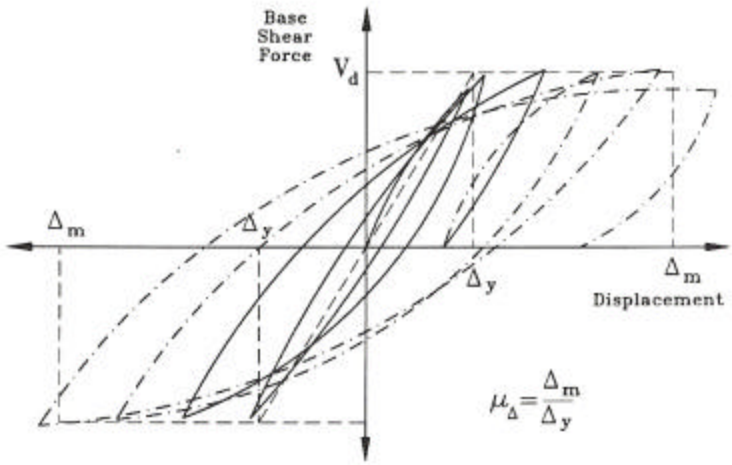

Fig. 8 Lateral load-displacement relation (Priestley et al. 1996)

Based on the relation between shear strength and displacement ductility in Fig. 7, the shear strength model proposed by Sezen et al. (2004) is developed by introducing a ductility related factor *k* which is similarly used by other previously proposed models such as Priestley's approach (1994) and Caltrans in Section 2.1. To apply the term *k* to estimate shear strength of circular columns, it is assumed that displacement ductility influences the shear strength contributed by both concrete and transverse reinforcement. Concrete damage under cyclic loading causes the degradation of the strength supported

by both the transverse reinforcement and concrete (Sezen et al. 2004). In this study, therefore, it is reasonable to apply the ductility-related factor k equally to both contributions. The following equation indicates the shear strength model with the factor k as a variable to explain ductility-related strength degradations.

$$V_n = V_s + V_c = k\frac{p}{2}\frac{A_{sh} f_y D'}{s} + k\left(\frac{0.5\sqrt{f'_c}}{a/d}\sqrt{1+\frac{P}{0.5\sqrt{f'c}A_g}}\right)0.8A_g \quad \text{(MPa)} \qquad (22)$$

Since the shear model of Eq. (22) is defined by modifying and exploring Sezen's approach (2004), it also seems reasonable to use the factor k defined by Sezen et al. (2004) as a primary reference. The factor k to estimate the shear strength of circular columns is thus defined by the following:

i. $k = 1$ where displacement ductility is smaller than 2.

ii. $k =$ vary linearly where displacement ductility is between 2 and 6.

iii. $k = 0.7$ where displacement ductility is larger than 6.

3.5 COMPARISON OF CALCULATED AND MEASURED STRENGTH

To validate the cited models in this study, columns included in Table 1 are analyzed. Results are presented in the form of graphs relating the experimentally recorded strength to the strength obtained from models reviewed in Section 2.1 and 3.4. As shown in Fig. 9, the shear strength calculated by Eq. (22) shows reasonably close values to the measured shear strength in terms of parameters including the range of displacement ductility, aspect ratio, axial load ratio, and transverse reinforcement index.

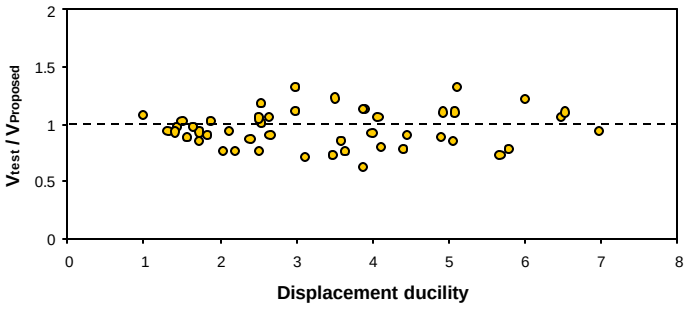

(a)

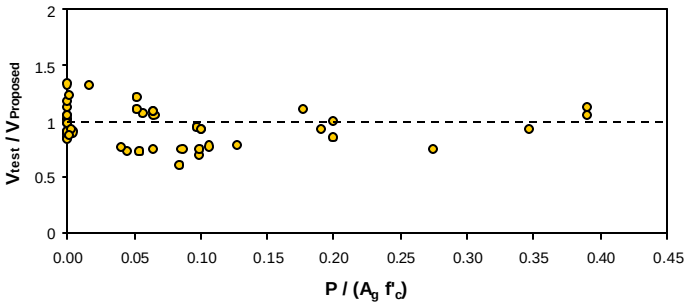

(b)

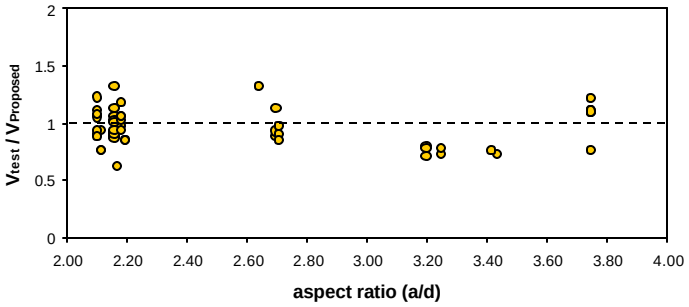

(c)

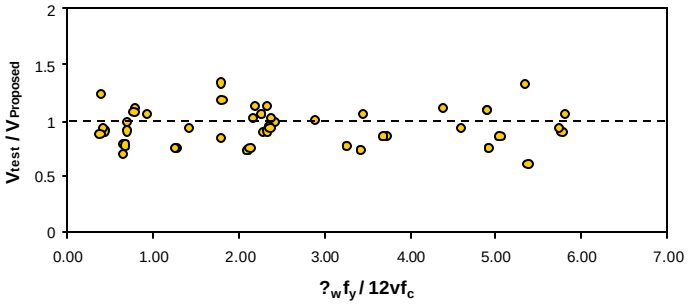

(d)

Fig. 9 Variation of measured to calculated strength ratio as a function of (a) displacement ductility; (b) axial load ratio;(c) aspect ratio; and, (d) transverse reinforcement index

Figs. 10, 11, 12, 13, and 14 show the ratio of measured to calculated shear strength as a function of key parameters for the models from ACI 318-3005 (2005); ATC-32; ASCE/ACI-426; Caltrans; and Priestley et al. (1994), respectively. It is observed that shear strengths calculated by ACI 318-2005 in addition to the model of Eq. (22) are close to measured shear strengths compared with other models. This effect also coincides with the result that ACI-318 and the model of Eq. (22) correlate well with the parameters discussed in Section 3.1. However, note that the vertical scales in the figure of Caltrans and Priestley et al. (1994) are relatively more expanded among available models for displacement ductility of 2.0 and larger. The main reason of this scatter is that V_c of some test columns calculated by either Caltrans or Priestley's models is smaller than that of other models. It thus concludes that ACI-318 and the model of Eq. (22) may be suitable as design and assessment tools for columns having similar configuration.

Table 2 summarizes statistical evaluation of the ratio of measured to calculated shear strength models with displacement ductility. This result shows that the model proposed by Sezen et al. (2004) provides slightly better statistical correlation with experimental data.

	The model of Eq. (22)	ACI 318	ATC-32	ASCE/ACI 426	Caltrans	Priestley et al. (1994)
Max	1.327	1.315	1.802	1.702	4.109	2.707
Min	0.613	0.270	0.341	0.280	0.227	0.242
Avg	0.944	0.905	0.980	0.903	1.189	1.286
*Stdv	0.165	0.273	0.312	0.325	0.598	0.572
*COV	0.175	0.301	0.319	0.360	0.503	0.445

Stdv: standard deviation
COV coefficient of variation

Table 2 Ratio of measured to calculated shear strength for different models versus displacement ductility

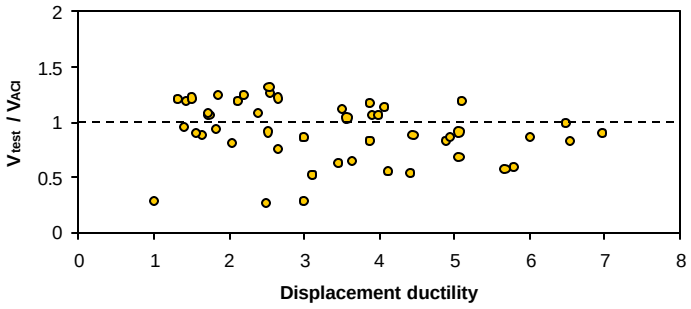

(a)

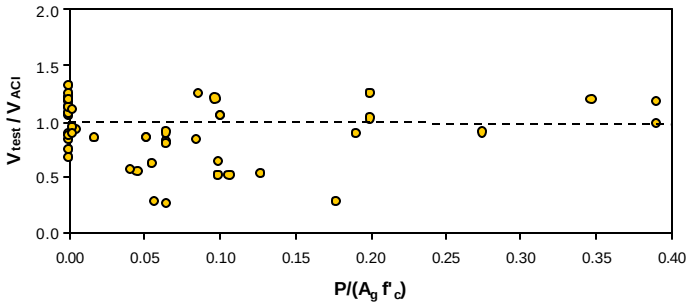

(b)

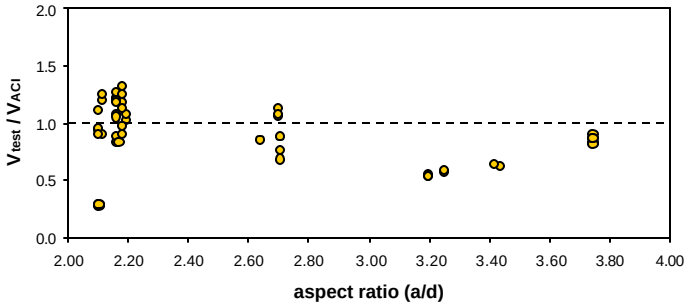

(c)

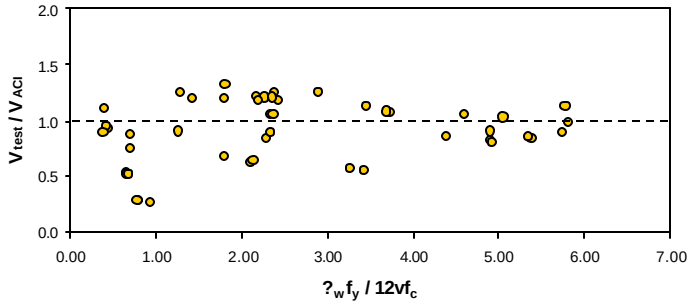

(d)

Fig. 10 Variation of V_{test} / V_{ACI} as a function of (a) displacement ductility; (b) axial load ratio; (c) aspect ratio; and (d) transverse reinforcement index

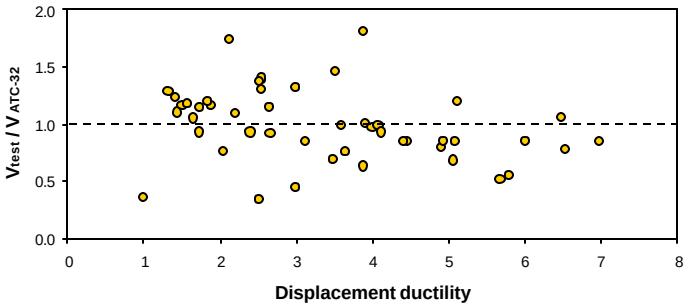

(a)

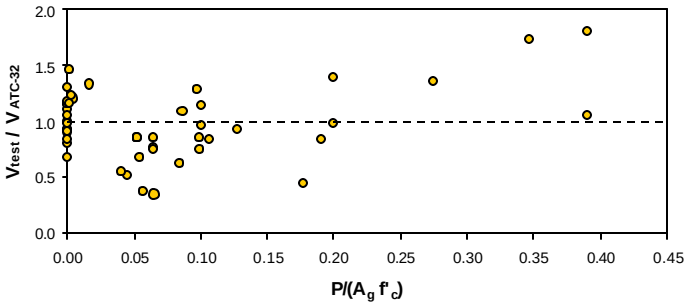

(b)

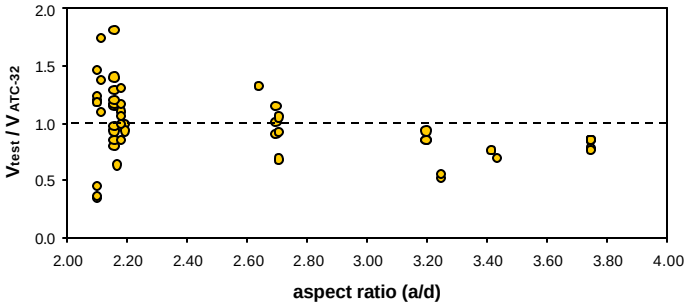

(c)

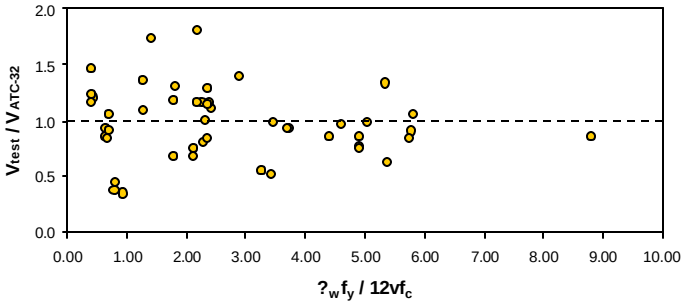

(d)

Fig. 11 Variation of V_{test} / V_{ATC-32} as a function of (a) displacement ductility; (b) axial load ratio; (c) aspect ratio; and (d) transverse reinforcement index

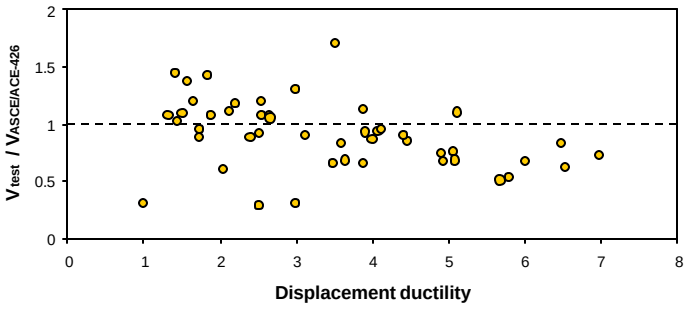

(a)

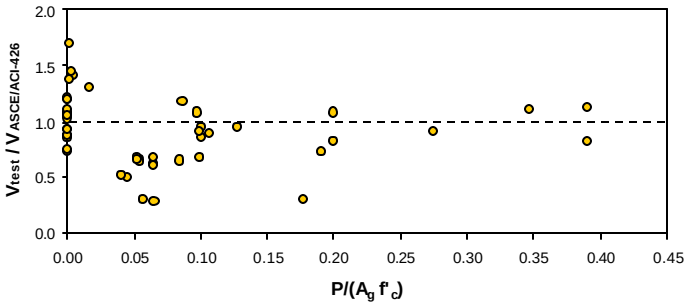

(b)

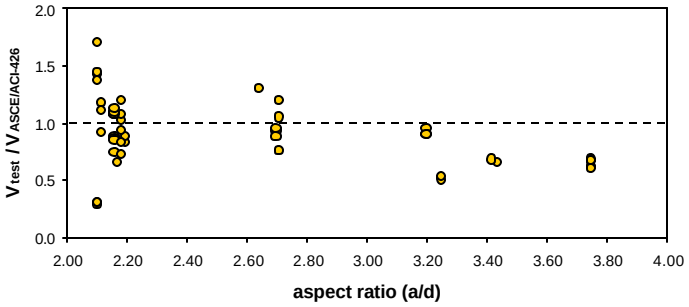

(c)

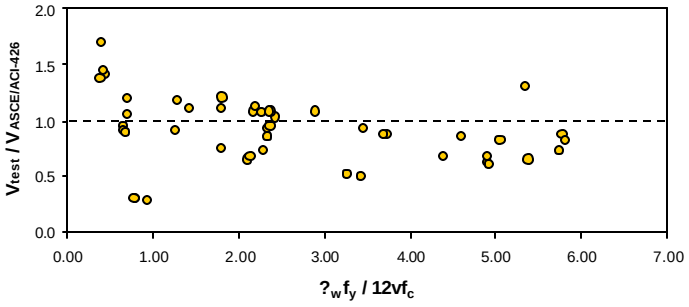

(d)

Fig. 12 Variation of $V_{test} / V_{ASCE/ACI-426}$ as a function of (a) displacement ductility; (b) axial load ratio; (c) aspect ratio; and (d) transverse reinforcement index

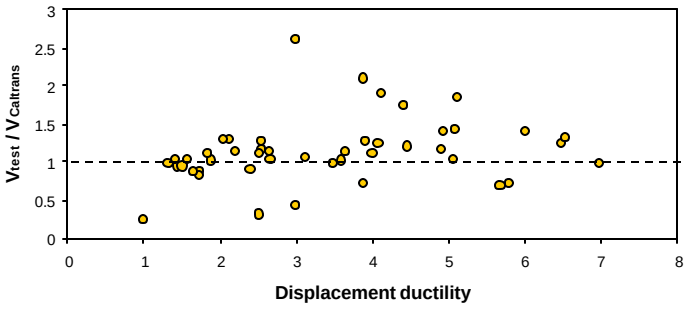

(a)

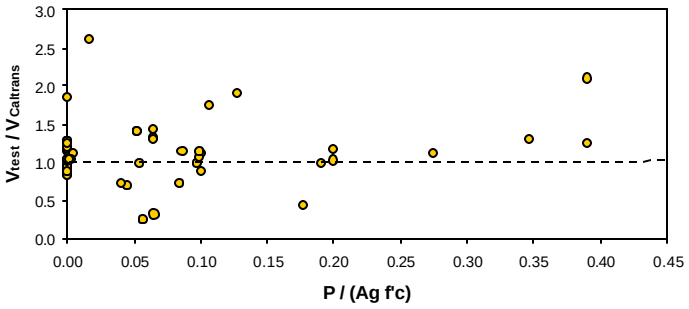

(b)

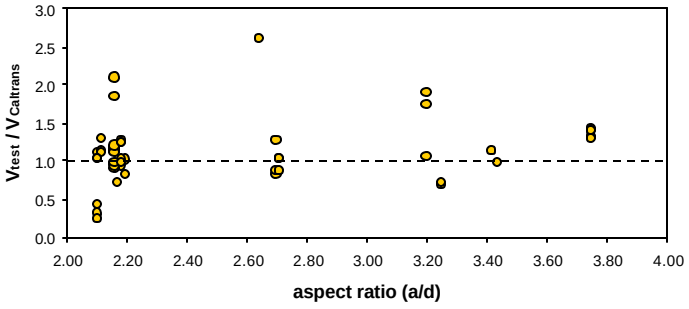

(c)

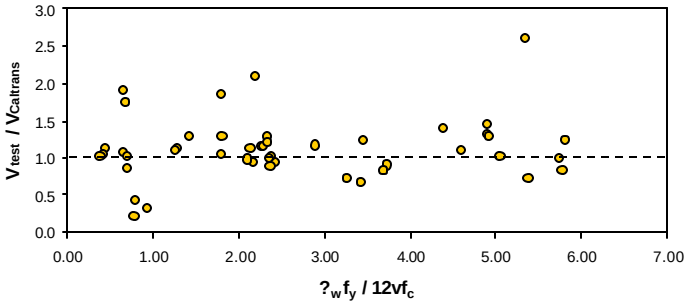

(d)

Fig. 13 Variation of $V_{test} / V_{Caltrans}$ as a function of (a) displacement ductility; (b) axial load ratio; (c) aspect ratio; and (d) transverse reinforcement index

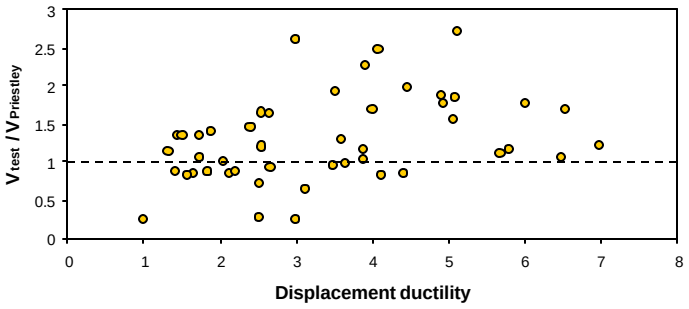

(a)

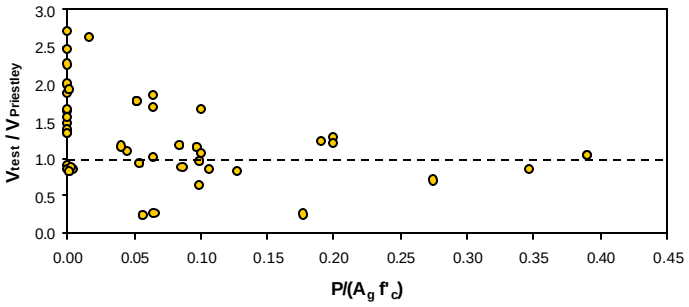

(b)

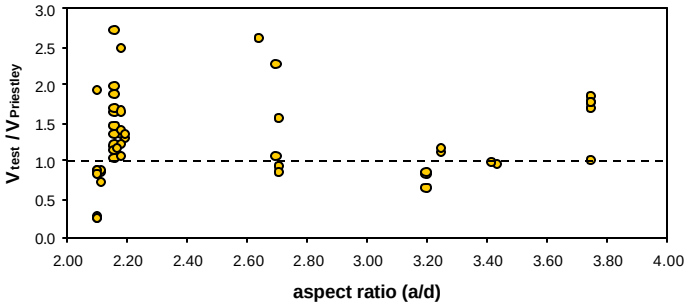

(c)

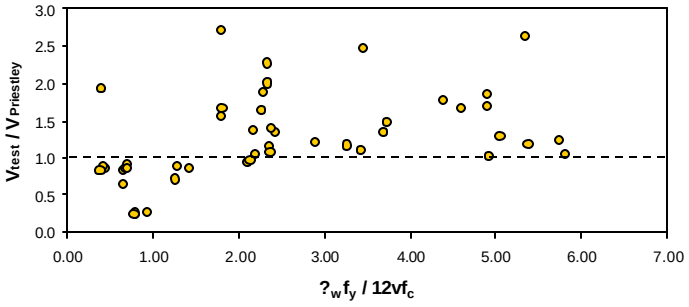

(d)

Fig. 14 Variation of $V_{test} / V_{Priestley}$ as a function of (a) displacement ductility; (b) axial load ratio; (c) aspect ratio; and (d) transverse reinforcement index

CHAPTER 4

CONCLUSIONS

Key parameters affecting the shear strength of circular reinforced concrete columns are examined based on the statistical evaluation of experimental data from numerous column tests. Results indicates that the shear strength is correlated with several parameters including the column aspect ratio, axial load, amount of transverse reinforcement, and deformation ductility demand. The previously proposed shear strength models are evaluated by considering the effects of these parameters. The shear strength model proposed by Sezen et al. (2004) is a combination of concrete and transverse reinforcement contributions and a function of displacement ductility demand. Also, the examination of existing design equations such as Caltrans and Priestley's approach (1994) reveals relatively wide difference from results obtained from laboratory tests. On the other hand, both Sezen's approach (2004) and ACI-318 (2005) fairly correlate with parameters examined in this research. In consideration of displacement ductility, the result shows that the model of Eq. (22) provides marginally better statistical correlation with experimental data. However, the model of Eq. (22) is estimated, given that the data of displacement ductility is known; so, note that it should not be used to estimate

displacement ductility based on shear strengths. To obtain the displacement ductility demand of the circular column, it would be necessary to employ further experimental and mathematical methods. The shear strength model proposed by Sezen et al. (2004) is then to estimate approximately the shear strength of circular columns having similar configuration only if the displacement ductility demand is known.

NOTATION

A_g = gross area of section;

A_v = transverse reinforcement area within a spacing, s in the loading direction;

A_e = effective area, taken as 0.8 A_g

A_{sp} = cross section area of spiral

a = shear span (distance from maximum moment section to point of inflection)

c = neutral axis depth

D = diameter of column section

D'or D_{sp} = diameter of center-to-center hoop or spiral

d = effective depth

d_h = diameter of the hoop or spiral

Δ_y = yield displacement

Δ_m = ultimate displacement

f'_c = compressive strength of concrete

f_y, f_{yh} = transverse reinforcement yield strength

f_{yl} = longitudinal reinforcement yield strength

k = factor relating to the concrete or transverse reinforcement capacity to displacement ductility

μ_d, m_Δ = displacement ductility

P = axial load

r_w = spiral reinforcement content

$r_t = A_s / b_w d$; tension steel ratio

r_l = longitudinal reinforcement ratio

V_n = nominal shear strength

V_s = nominal shear strength carried by transverse reinforcement

V_c = nominal shear strength carried by concrete

V_p = nominal shear strength enhancement provided by axial compression

V_{test} = experimental shear strength

BIBLIOGRAPHY

American Concrete Institute (ACI). (2005). "Building code requirements for structural concrete," ACI committee 318, Farmington Hills, Mich.

Applied Technology Council, "Improved Seismic Design Criteria for California Bridges: Provisional Recommendation," Report No. ATC-32, Readwood City, Calif.,1996.

Caltrans Memo to Designers 20-4, Attachment B, "Earthquake Retrofit Analysis for Single Column Bents," Aug. 1996.

Ghee, A. B., Priestley, M.J.N., and Paulay, T., "Seismic Shear Strength of Circular Reinforced Concrete Columns," ACI Structural Journal, January-February 1989, p. 45-59.

Ghee, A. B., Priestley, M.J.N., and Paulay, T., "Seismic Shear Strength of Circular Bridge Piers," Report 85-5, Department of Civil Engineering, University of Canterbury, Christchurch, New Zealand, July 1985.

Hamilton, C. H., Pardoen, G. C., and Kazanjy, R. P., "Experimental Testing of Bridge Columns Subjected to Reversed-Cyclic and Pulse-type Loading Histories," Report 2001-03, Civil Engineering Technical Report Series, University of California, Irvine, 2002.

Kawashima Earthquake Engineering Laboratory, "Cyclic Loading Test Data of Reinforced Concrete Bridge Piers," Tokyo Institute of Technology, http://seismic.cv.titeh.ac.jp

Kowalsky, M. J. and Priestley, M. J. N., "Improved Analytical Model for Shear Strength of Circular Reinforced Concrete Columns in Seismic Regions," ACI

Structural Journal. May-June 2000, pp. 388-396.

McDaniel, C, "Scale Effects on the Shear Strength of Circular Reinforced Concrete Columns," University of California, San Diego, 1997.

Nelson, J. M., "Damage Model Calibration for Reinforced Concrete Columns," Master's Thesis, Department of Civil and Environmental Engineering, University of Washington, 2000.

Ohtaki, T., Benzoni, G., and Priestley M. J. N., "Seismic Performance of a Full-Scale Bridge Column - As Built and As Repaired," University of California, San Diego, Structural Systems Research Project, Report No. SSRP-96/07, November, 1996.

Petrovski, J. and Ristic, D., "Reversed Cyclic Loading Test of Bridge Column Models," Report IZIIZ 84-164, Institute of Earthquake Engineering and Engineering Seismology, September 1984, 62 pages.

Priestley, M. J. N., Verma, R., and Xiao, Y., (1994). "Seismic Shear Strength of Reinforced Concrete Columns," J. Strut. Eng, 120(8), 2310-2239.

Priestley, M. J. N., Seible, F., and Calvi, G. M., (1996). "Seismic Design and Retrofit of Bridges," John Wiley & Sons, Inc., New York, 686 pp.

Priestley, M. J. N, Benzoni, G., "Seismic Performance of Circular Columns with Low Longitudinal Reinforcement Ratios," ACI Structural Journal, vol. 93, No.4, July-August, 1996, pp. 474-485

Standard New Zealand, 1995, "Design of Concrete Structures," NZS 3101, Wellington, New Zealand.

Sezen, H. and Moehle, Jack P., "Shear Strength Model for Lightly Reinforced Concrete

Columns," ACI Structural Journal, November 2004, p. 1692-1703.

Sritharan, S., Priestley, M. J. N., and Seible, F., "Seismic Response of Column/Cap Beam Tee Connections with Cap Beam Prestressing," University of California, San Diego, Structural Systems Research Project, Report No. SSRP-96/09, December 1996.

The Department of Civil Engineering at University of Washington, "Structural Performance Database", www.ce.washingtong.edu/~peera1/

Verma, R., Priestley, M. J. N., and Seible, F., "Assessment of Seismic Response and Steel Jacket Retrofit of Squat Circular Reinforced Concrete Bridge Columns," Report No. SSRP-92/05, UCSD, June 1993.

Vu, N. D., Priestley, M. J. N., Seible, F., and Benzoni, G., "Seismic Response of Well Confined Circular Reinforced Concrete Columns with Low Aspect Ratios," 5th-Caltrans Seismic Research Workshop, 1998.

Wong, Y.L., Paulay, T., and Priestley, M.J.N., "Squat Circular Bridge Piers Under Multi-Directional Seismic Attack", Report 90-4, Department of Civil Engineering, University of Canterbury, Christchurch, New Zealand, October 1990, 264 pages.

Wong, Y.L., Paulay, T., and Priestley, M. J. N. (1993). "Response of Circular Reinforced Concrete Columns to Multi-Directional Seismic Attack," ACI Structural Journal, Vol 90, No.2, pp. 180-191.

APPENDIX

A. TEST COLUMN DIMENSIONS AND TEST SETUPS

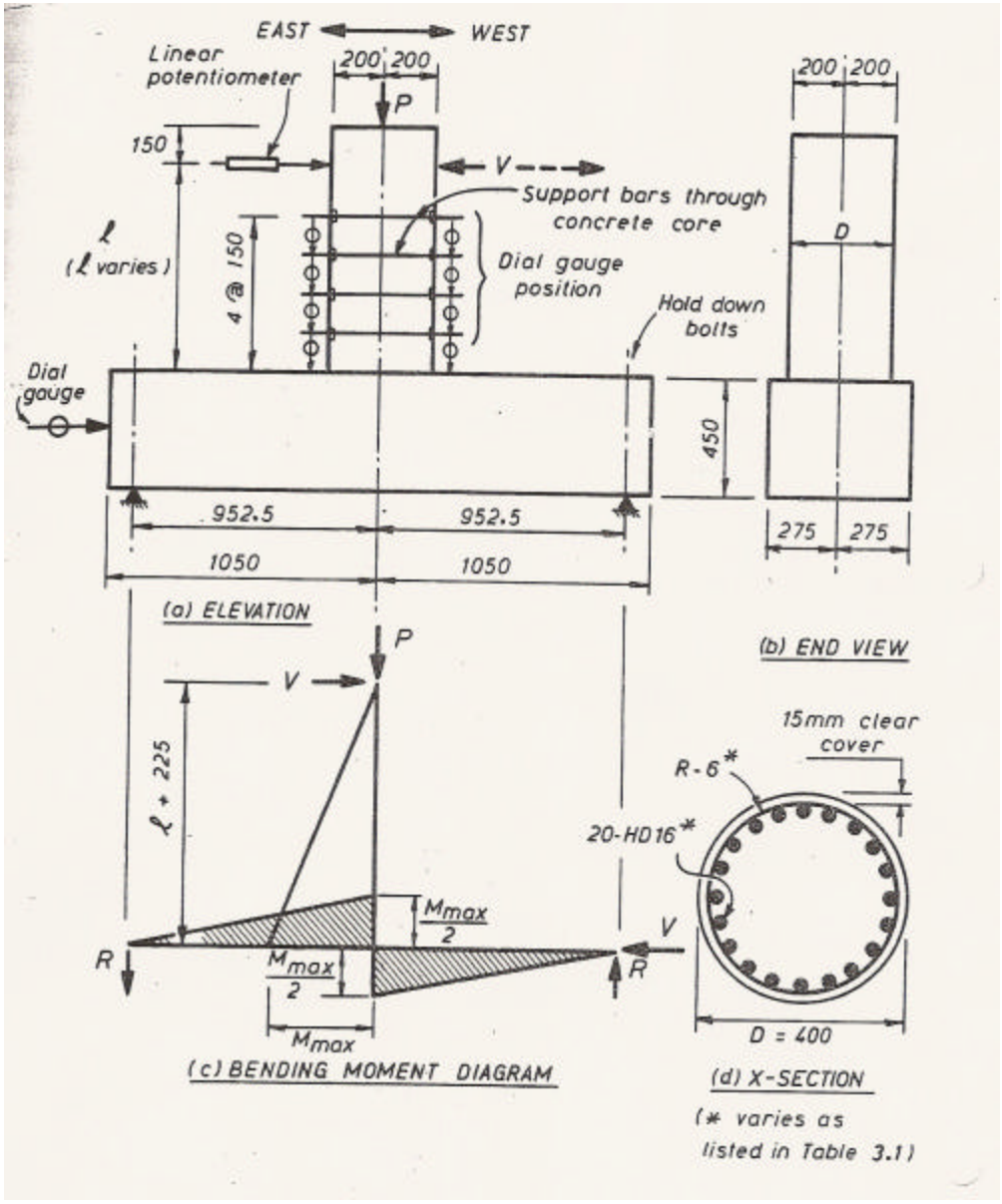

Fig. A.1 Column Detail of Ang's test units (Ang et al. 1985)

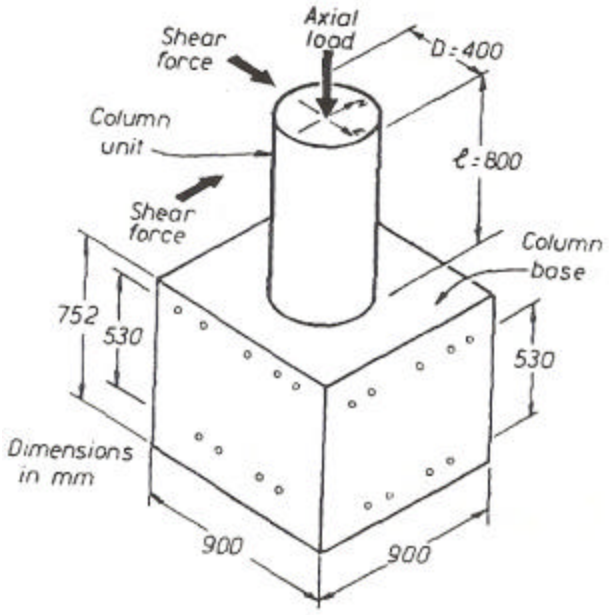

Fig. A.2 Dimensions and loading test columns (Wong et al. 1993)

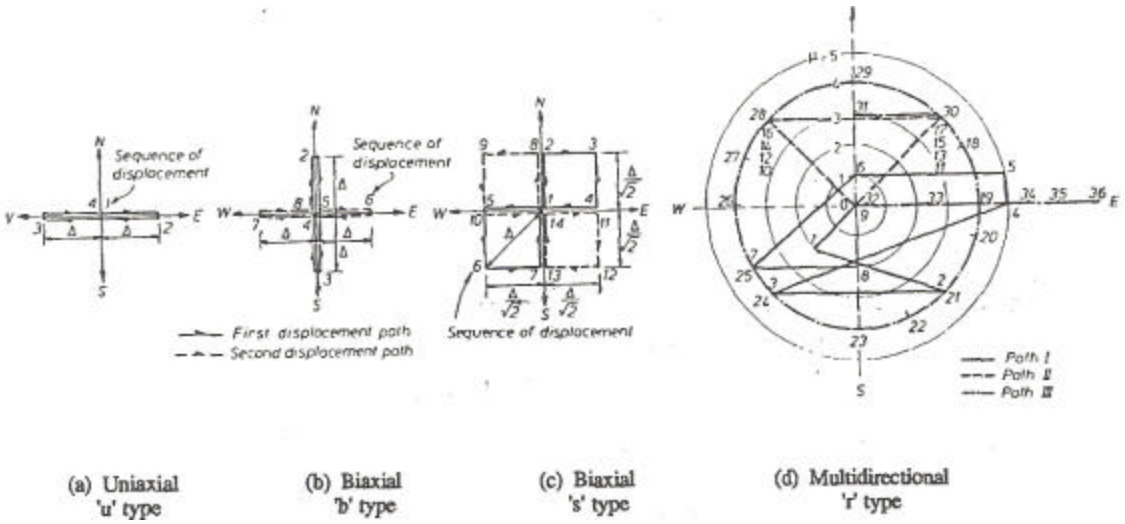

Fig. A.3 Different displacement patterns used in testing (Wong et al. 1993)

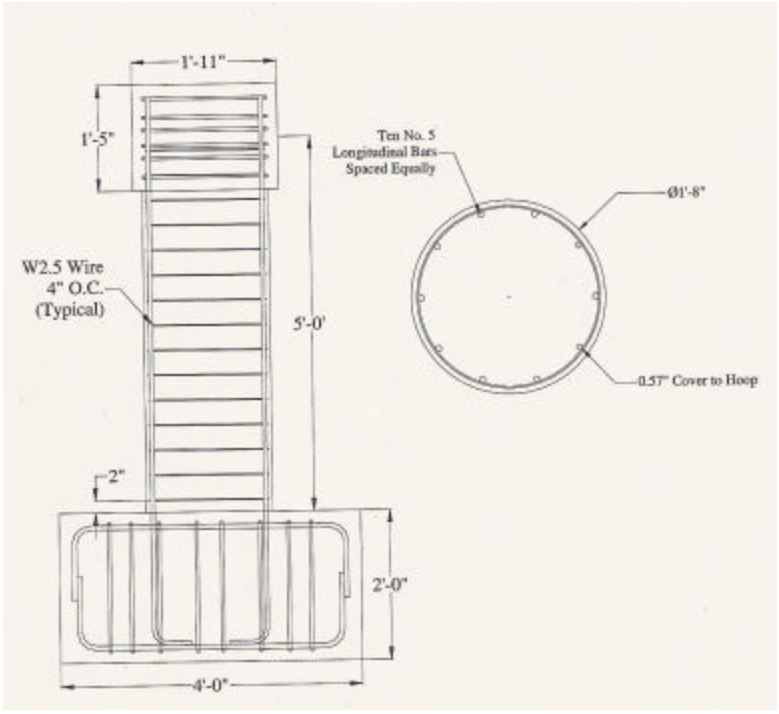

Fig. A.4 Test Column Geometry and Reinforcement (Nelson 2000)

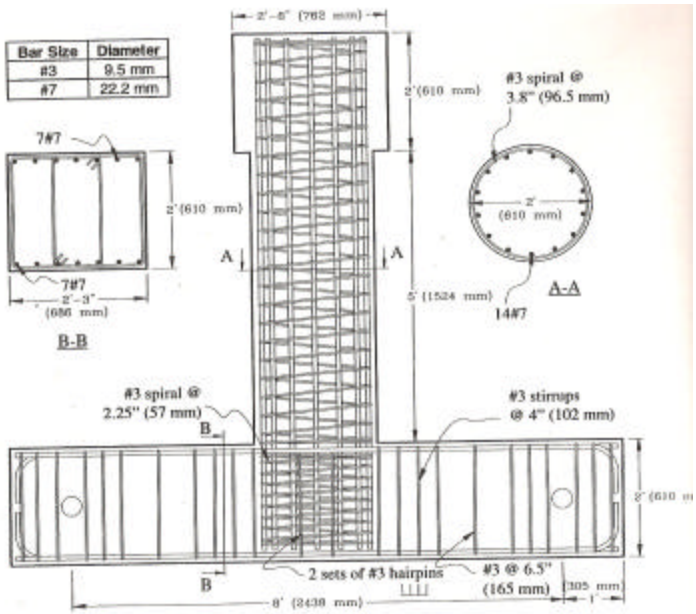

(a) Unit IC1

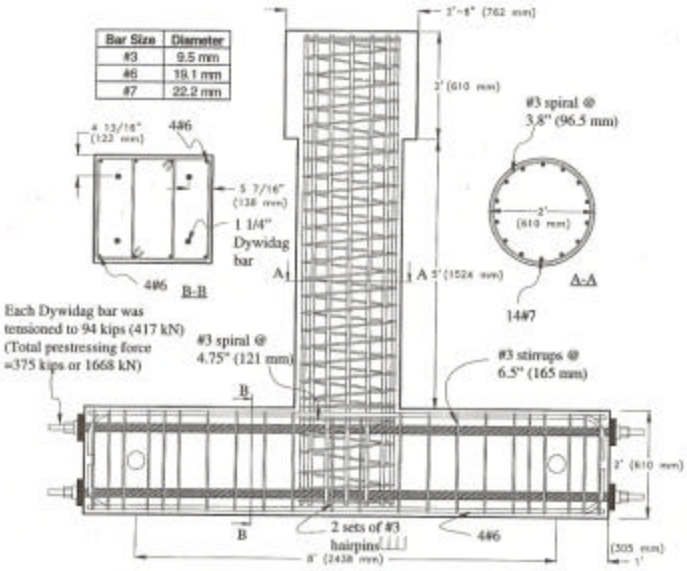

(b) Unit IC2

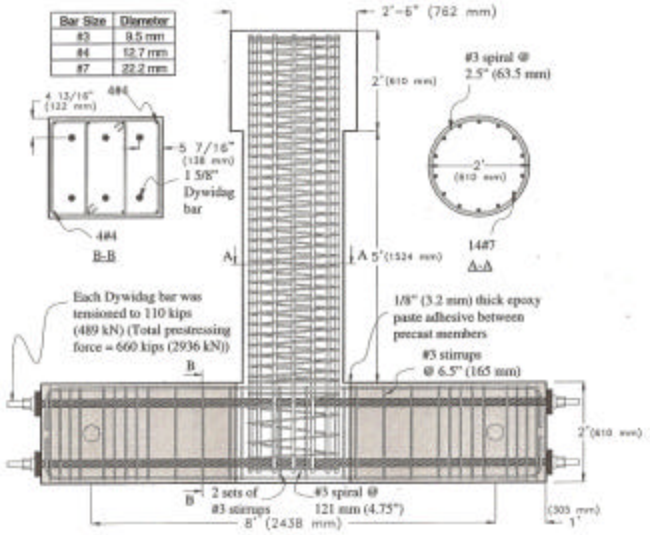

(c) Unit IC3

Fig. A.5 Column Details of (a) IC1; (b) IC2; and IC3 (Sritharan et al. 1996)

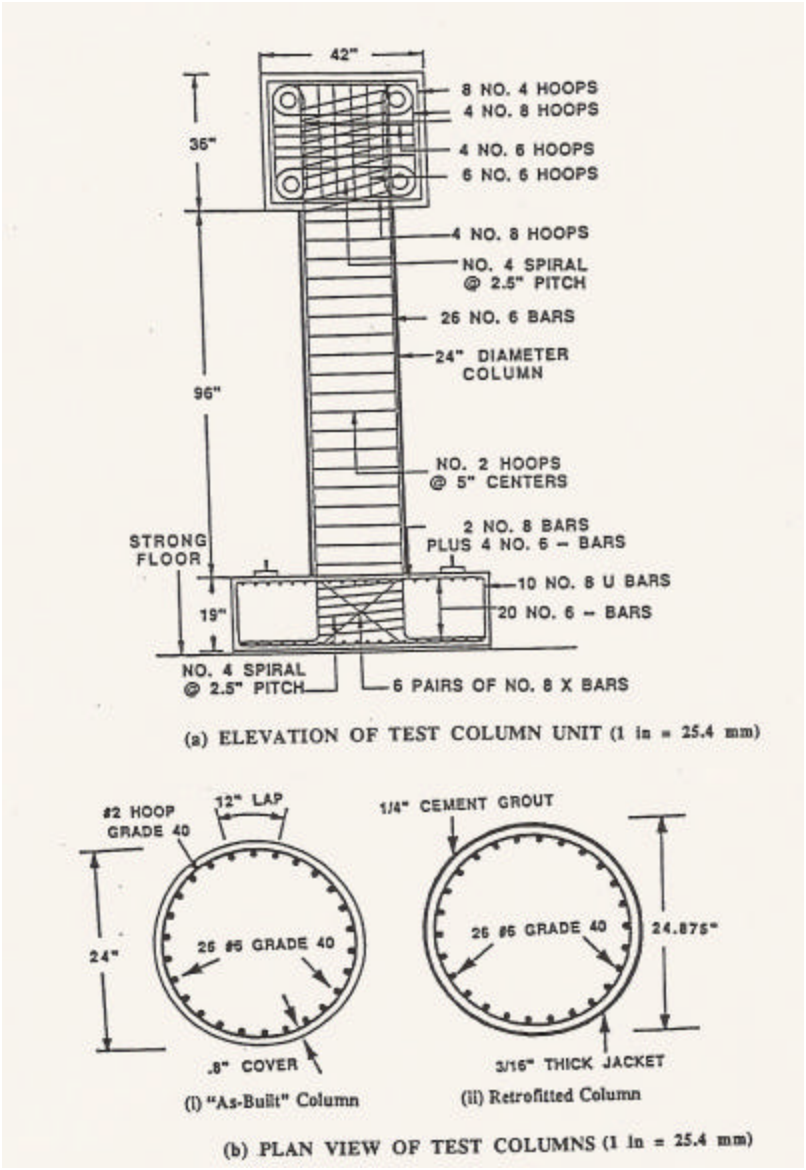

Fig. A.6 Detail of Verma's Column Units (Verma et al. 1993)

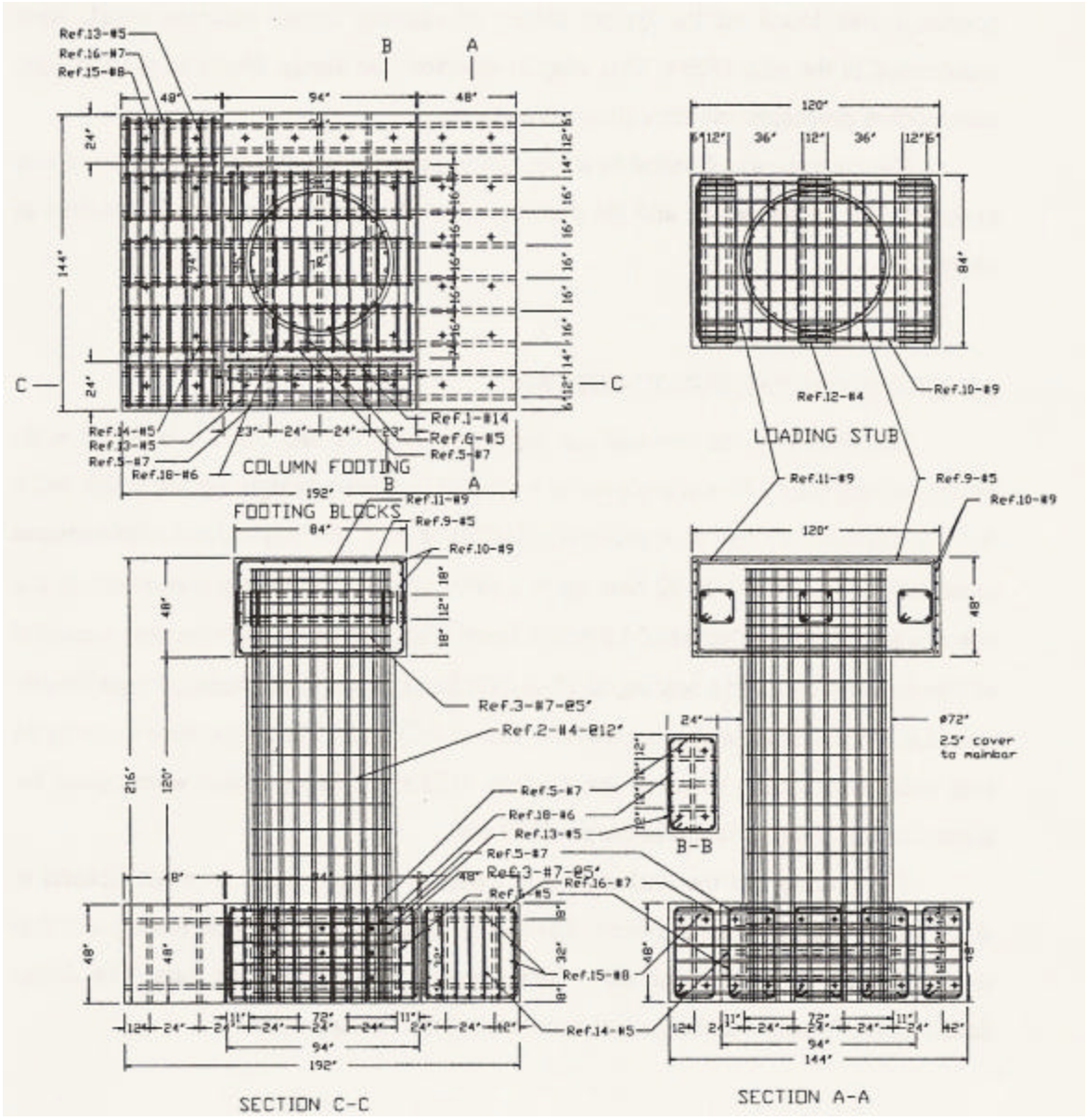

Fig. A.7 Column detail of L1 (Ohtaki et al. 1996)

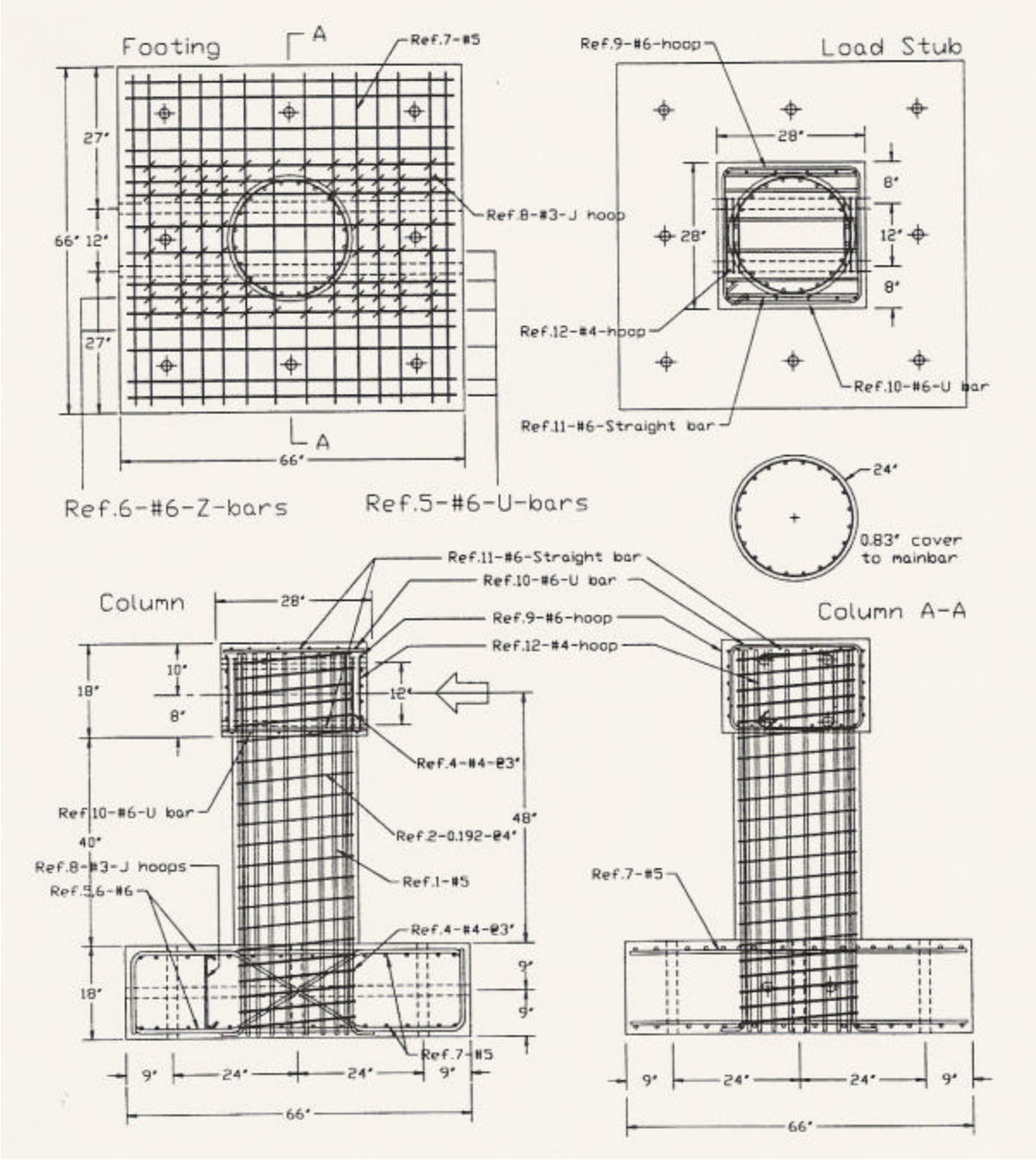

Fig. A.8 Column detail of S1, S1-2, and S3 (McDaniel 1997)

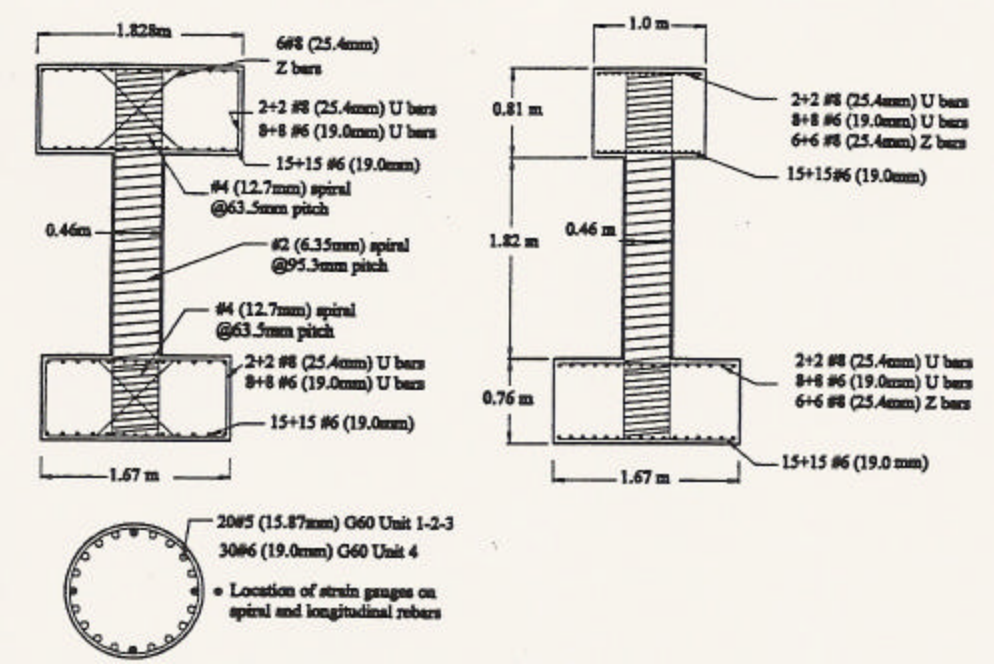

Fig. A.9 Column detail of CS1 & CS2 (left) and CS3 & CS4 (right) (Benzoni et at. 1996)

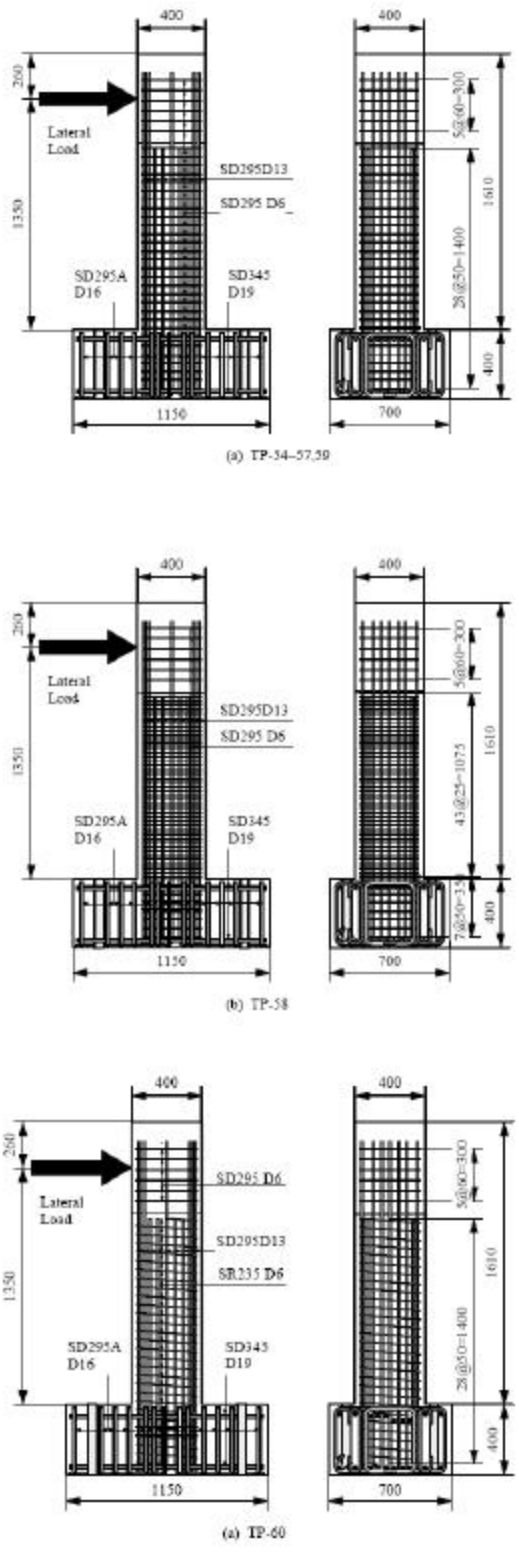

Fig. A.10 Column detail of test units (Kawashima Lab.)

	ACI				ATC-32				ASCE/ACI 426				Caltran			
	Vc (kN)	Vs (kN)	Vn (kN)	V_{test}/V_n	Vc (kN)	Vs (kN)	Vn (kN)	V_{test}/V_n	Vc (kN)	Vs (kN)	Vn (kN)	V_{test}/V_n	Vc (kN)	Vs (kN)	Vn (kN)	V_{test}/V_n
No.1	150.9	114.7	265.5	1.209	102.8	176.8	279.6	1.148	123.1	176.8	299.9	1.070	104.1	176.8	280.8	1.143
No.2	150.2	114.7	264.9	0.834	102.4	176.8	279.1	0.792	122.6	176.8	299.4	0.738	15.3	176.8	192.1	1.151
No.3	147.8	114.7	262.5	1.051	100.7	176.8	277.5	0.995	120.6	176.8	297.4	0.928	38.9	176.8	215.6	1.280
No.4	134.8	110.4	245.2	1.179	92.9	170.1	263.0	1.099	111.2	170.1	281.3	1.027	139.0	170.1	309.1	0.935
No.5	137.4	172.0	309.4	1.070	93.6	265.1	358.8	0.923	112.1	265.1	377.3	0.877	106.4	265.1	371.5	0.891
No.7	133.8	97.6	231.4	1.215	91.2	150.3	241.5	1.163	109.2	150.3	259.6	1.083	150.6	150.3	300.9	0.934
No,9	134.7	260.1	394.8	1.127	91.8	400.9	492.7	0.903	109.9	400.9	510.9	0.871	137.4	400.9	538.4	0.827
No.10	196.6	228.4	425.0	1.029	93.8	351.9	445.7	0.981	179.7	351.9	531.6	0.823	75.7	351.9	427.6	1.023
No.11	193.0	130.1	323.1	1.260	91.8	200.5	292.3	1.392	175.9	200.5	376.3	1.081	148.6	200.5	349.0	1.166
No.13	187.1	228.0	415.1	1.051	101.0	351.4	452.4	0.964	157.3	351.4	508.6	0.858	43.1	351.4	394.5	1.106
No.14	141.5	112.8	254.2	1.243	97.5	175.7	273.1	1.157	116.7	175.7	292.4	1.081	136.7	175.7	312.4	1.012
No.15	145.3	114.0	259.3	0.887	99.0	175.7	274.7	0.837	96.0	175.7	271.7	0.847	14.8	175.7	190.5	1.207
No.16	179.5	114.0	293.5	1.200	98.5	175.7	274.2	1.285	152.3	175.7	328.0	1.074	183.1	175.7	358.8	0.982
No.17	180.1	114.0	294.1	1.062	98.3	175.7	274.0	1.140	153.1	175.7	328.8	0.950	179.4	175.7	355.1	0.880
No.21	141.9	85.5	227.4	1.192	96.7	131.8	228.5	1.186	115.9	131.8	247.6	1.094	14.5	131.8	146.2	1.853
No.22	135.5	81.2	216.7	1.315	93.3	125.2	218.5	1.304	111.8	125.2	236.9	1.203	97.0	125.2	222.1	1.283
No.23	137.7	171.3	309.1	1.077	95.4	263.9	359.4	0.927	114.3	263.9	378.2	0.880	142.8	263.9	406.8	0.819
No.24	140.2	162.5	302.7	1.127	96.6	250.3	346.9	0.983	115.7	250.3	366.0	0.932	26.4	250.3	276.8	1.232
Col1	457.4	67.6	525.0	0.539	203.1	103.8	306.9	0.922	193.9	103.8	297.7	0.951	45.6	103.8	149.3	1.895
Col3	426.9	67.6	494.5	0.526	204.5	103.8	308.3	0.843	183.1	103.8	286.9	0.906	141.4	103.8	245.1	1.061
Col4	410.5	67.6	478.1	0.527	196.7	103.8	300.4	0.839	179.4	103.8	283.1	0.890	41.4	103.8	145.2	1.736
UCI 3	153.5	35.3	188.8	0.757	101.8	55.2	157.0	0.911	81.9	55.2	137.1	1.043	84.2	55.2	139.4	1.026
UCI 4	153.5	35.3	188.8	0.869	101.8	55.2	157.0	1.045	81.9	55.2	137.1	1.196	135.8	55.2	191.0	0.859
UCI 5	155.5	95.4	250.8	0.678	103.1	149.1	252.2	0.674	76.8	149.1	225.9	0.752	15.4	149.1	164.5	1.033
No.1	228.8	288.2	517.0	0.892	103.5	444.1	547.7	0.842	194.6	444.1	638.7	0.722	23.2	444.1	467.4	0.986
No.2	306.5	109.7	416.2	1.175	102.2	169.1	271.4	1.802	265.4	169.1	434.5	1.125	64.2	169.1	233.3	2.096
No.3	303.2	288.2	591.4	0.979	102.2	444.1	546.4	1.060	265.4	444.1	709.5	0.816	22.9	444.1	467.1	1.240
M2E1	91.4	47.4	138.8	0.620	59.3	66.8	126.1	0.682	65.0	66.8	131.8	0.653	21.1	66.8	87.9	0.978
M2E2	97.8	47.4	145.2	0.641	58.0	66.8	124.8	0.745	71.1	66.8	137.9	0.674	16.5	66.8	83.3	1.116
NH5	148.0	335.0	482.9	0.835	129.9	511.0	640.9	0.629	108.3	511.0	619.3	0.651	42.9	511.0	553.9	0.728
IC1	340.9	350.8	691.7	0.560	211.7	536.8	748.5	0.517	233.0	536.8	769.8	0.503	34.9	536.8	571.7	0.677
IC2	357.8	350.8	708.6	0.580	222.2	536.8	759.0	0.541	241.9	536.8	778.7	0.528	36.7	536.8	573.5	0.717
IC3	294.1	214.0	508.1	0.852	190.4	136.4	326.7	1.325	197.2	136.4	333.5	1.298	29.4	136.4	165.7	2.613
v1	374.8	103.7	478.5	0.270	217.2	161.6	378.8	0.341	299.3	161.6	460.9	0.280	253.7	161.6	415.3	0.311
v 3	496.7	93.7	590.4	0.279	229.0	146.1	375.1	0.440	403.8	146.1	549.8	0.300	240.4	146.1	386.4	0.427
v 5	402.9	93.7	496.6	0.278	233.5	146.1	379.6	0.364	314.6	146.1	460.7	0.300	461.2	146.1	607.2	0.227
L1	2908	431.9	3340	0.929	1909	667.1	2576	1.205	1533	667.1	2200	1.411	2123	667.1	2790	1.112
CS1	309.0	105.6	414.6	1.189	120.3	163.0	283.3	1.740	280.4	163.0	443.5	1.112	219.0	163.0	382.0	1.291
CS2	152.8	105.6	258.3	1.247	132.7	163.0	295.7	1.089	112.7	163.0	275.7	1.168	121.0	163.0	284.0	1.134
CS3	347.2	107.2	454.5	0.900	135.2	165.6	300.8	1.360	281.7	165.6	447.3	0.914	205.8	165.6	371.4	1.101
S1	322.3	43.1	365.4	1.111	212.9	66.8	279.6	1.452	171.8	66.8	238.6	1.702	32.0	66.8	98.8	4.109
S1-2	305.6	43.1	348.7	0.952	201.9	66.8	268.7	1.236	163.1	66.8	229.8	1.444	254.7	66.8	321.5	1.033
S2	329.8	43.1	372.9	0.890	217.8	66.8	284.6	1.167	175.8	66.8	242.5	1.369	257.4	66.8	324.2	1.024
*TP 54	125.1	152.5	277.5	0.822	79.5	217.3	296.7	0.768	151.9	217.3	369.2	0.618	131.3	217.3	348.6	1.308
*TP 55	125.1	152.5	277.5	0.903	79.5	217.3	296.7	0.844	151.9	217.3	369.2	0.679	131.3	217.3	348.6	1.437
*TP 57	124.8	152.5	277.3	0.808	79.3	217.3	296.6	0.755	151.7	217.3	368.9	0.607	131.0	217.3	348.3	1.286
*TP 60	139.3	127.1	266.4	0.862	88.5	181.1	269.6	0.851	163.9	181.1	345.0	0.665	146.3	181.1	327.3	1.402
*TP 61	139.3	127.1	266.4	0.858	88.5	181.1	269.6	0.848	163.9	181.1	345.0	0.663	146.3	181.1	327.3	1.397

Table A.1. Calculated Shear Strength based on available models

	Proposed Model [1]				Proposed Model[2]		
	V_{c_Prop} (kN)	Vs (kN)	Vn (kN)	V_{test}/V_n	*k* (kN)	kV_n (kN)	V_{test}/kV_n
No.1	142.7	176.8	319.5	1.00	0.94	298.7	1.07
No.2	142.2	176.8	318.9	0.693	0.71	226.4	0.976
No.3	111.9	176.8	288.6	0.956	0.81	233.5	1.18
No.4	127.6	170.1	297.7	0.971	1.0	297.7	0.971
No.5	130.0	265.1	395.1	0.838	0.96	379.3	0.873
No.7	126.6	150.3	277.0	1.01	1.0	277.0	1.01
No,9	102.0	400.9	502.9	0.885	1.0	502.9	0.885
No.10	230.4	351.9	582.3	0.751	0.84	490.3	0.892
No.11	227.5	200.5	428.0	0.951	0.95	404.4	1.01
No.13	208.2	351.4	559.5	0.780	0.80	447.6	0.975
No.14	133.9	175.7	309.5	1.02	1.0	309.5	1.02
No.15	137.5	175.7	313.2	0.734	0.75	236.1	0.974
No.16	200.0	175.7	375.7	0.938	1.0	375.7	0.938
No.17	160.9	175.7	336.6	0.928	1.0	336.6	0.928
No.21	134.3	131.8	266.1	1.02	0.69	183.6	1.48
No.22	128.2	125.2	253.3	1.12	0.95	239.7	1.19
No.23	130.3	263.9	394.3	0.845	1.0	394.3	0.845
No.24	132.7	250.3	383.0	0.890	0.79	303.3	1.12
Col1	324.1	103.8	427.8	0.661	0.79	336.7	0.840
Col3	301.9	103.8	405.7	0.641	0.89	360.2	0.722
Col4	293.8	103.8	397.5	0.634	0.76	301.3	0.836
UCI 3	112.7	55.20	167.9	0.852	0.93	156.8	0.912
UCI 4	112.7	55.20	167.9	0.977	1.0	167.9	0.977
UCI 5	114.1	149.1	263.2	0.646	0.69	182.7	0.931
No.1	259.9	444.1	704.0	0.655	0.60	422.4	1.09
No.2	339.8	169.1	508.9	0.961	0.81	413.3	1.18
No.3	336.2	444.1	780.3	0.742	0.60	468.2	1.24
M2E1	66.42	66.80	133.2	0.646	0.85	113.6	0.757
M2E2	74.89	66.80	141.7	0.656	0.84	118.5	0.785
NH5	254.2	511.0	765.3	0.527	0.81	622.2	0.648
IC1	239.3	536.8	776.1	0.528	0.63	490.5	0.836
IC2	249.2	536.8	786.0	0.548	0.62	488.1	0.883
IC3	233.5	136.4	369.8	1.22	0.90	332.8	1.36
verma 1	406.5	161.6	568.1	1.01	0.95	539.7	1.06
verma 3	571.8	146.1	717.9	1.02	0.90	646.1	1.14
verma 5	430.5	146.1	576.6	1.06	1.0	576.6	1.06
L1	2792	667.1	3459.2	0.897	1.0	3459	0.897
CS1	371.2	163.0	534.2	0.923	0.99	527.8	0.934
CS2	268.0	163.0	431.1	0.747	0.98	422.4	0.762
CS3	398.6	165.6	564.2	0.725	0.95	534.8	0.765
S1	307.1	66.79	373.9	1.09	0.85	317.4	1.28
S1-2	291.4	66.79	358.2	0.927	1.0	358.2	0.927
S2	314.2	66.79	380.9	0.872	1.0	380.9	0.872
*TP 54	80.49	217.3	297.8	0.766	0.60	178.7	1.28
*TP 55	80.49	217.3	297.8	0.841	0.69	206.3	1.21
*TP 57	80.34	217.3	297.6	0.753	1.0	296.2	0.756
*TP 60	87.92	181.1	269.0	0.853	0.71	189.9	1.21
*TP 61	87.92	181.1	269.0	0.850	0.60	161.4	1.42
Mean				0.845			1.00
STDV				0.164			0.189

[1] The factor *k* is not considered to estimate V_n

[2] The factor *k* is equal to 0.7 at displacement ducility larger than 6

Table A.2 Calculated shear strength based on proposed model.

B. FORCE-DISPLACEMENT HISTORIES

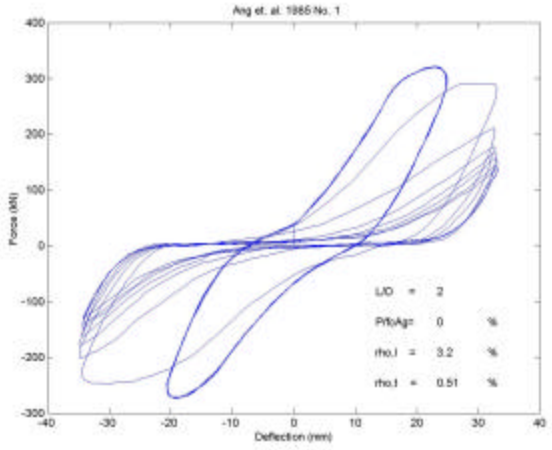

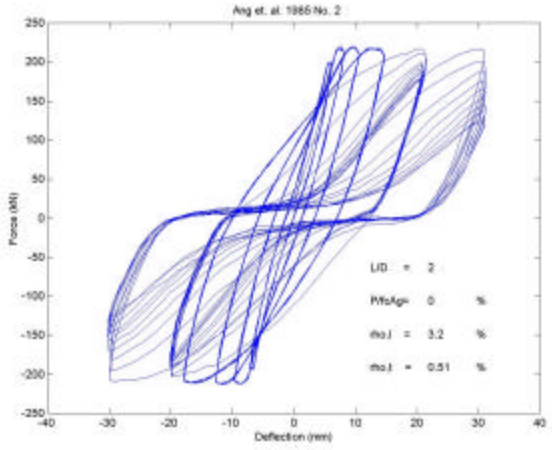

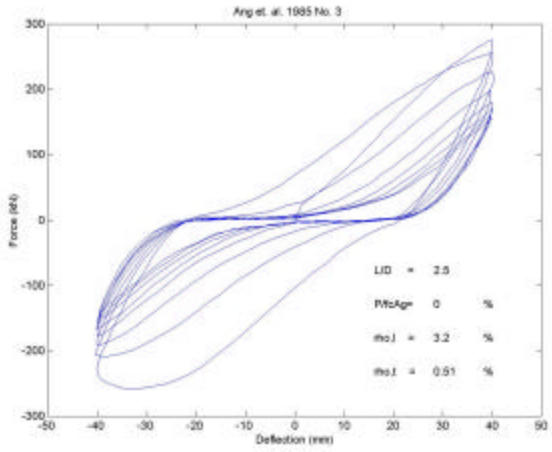

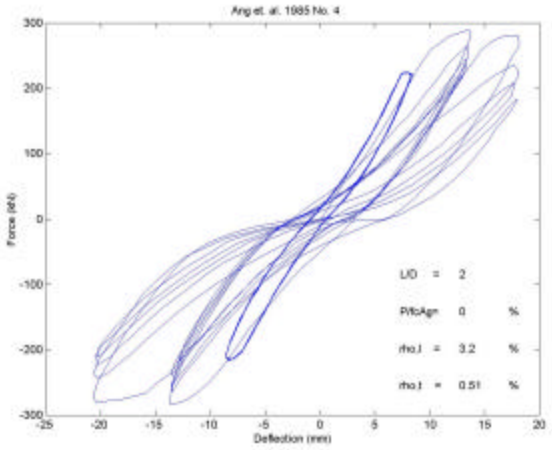

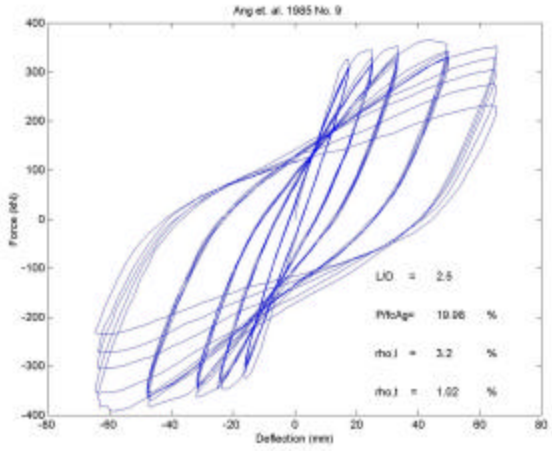

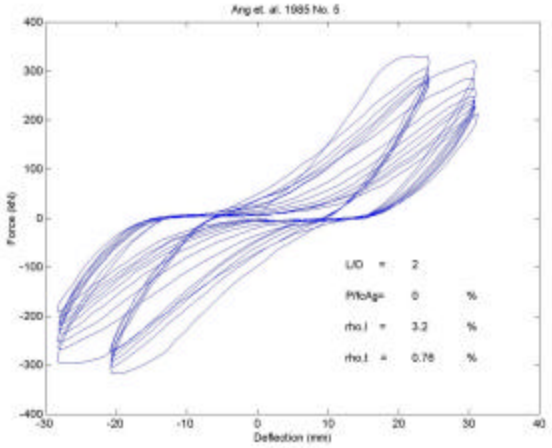

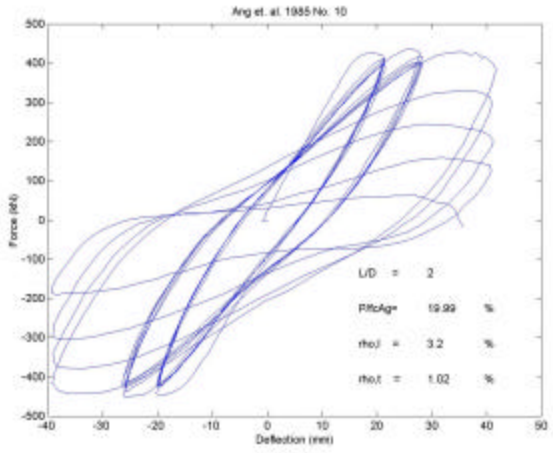
Ang et. al. 1985 No. 10
Force (kN)
Deflection (mm)
L/D = 2
P/fcAg= 19.99 %
rho.l = 3.2 %
rho.t = 1.02 %

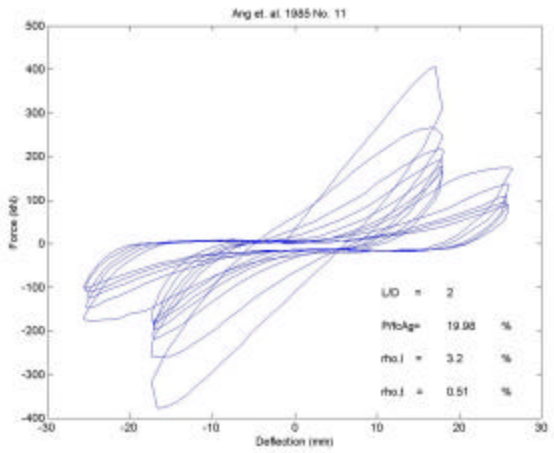
Ang et. al. 1985 No. 11
Force (kN)
Deflection (mm)
L/D = 2
P/fcAg= 19.98 %
rho.l = 3.2 %
rho.t = 0.51 %

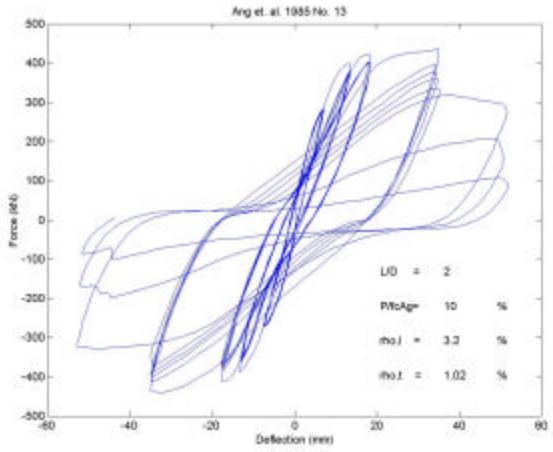
Ang et. al. 1985 No. 13
Force (kN)
Deflection (mm)
L/D = 2
P/fcAg= 10 %
rho.l = 3.2 %
rho.t = 1.02 %

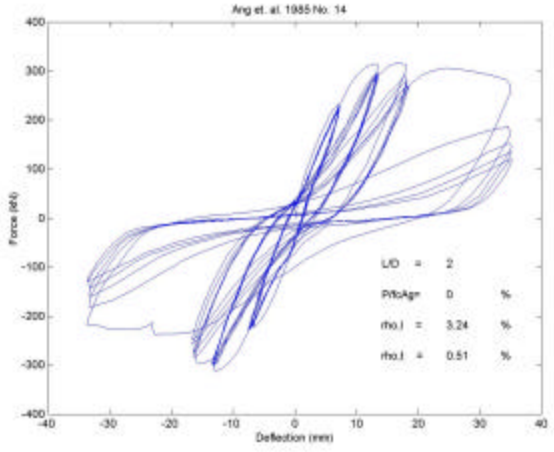
Ang et. al. 1985 No. 14
Force (kN)
Deflection (mm)
L/D = 2
P/fcAg= 0 %
rho.l = 3.24 %
rho.t = 0.51 %

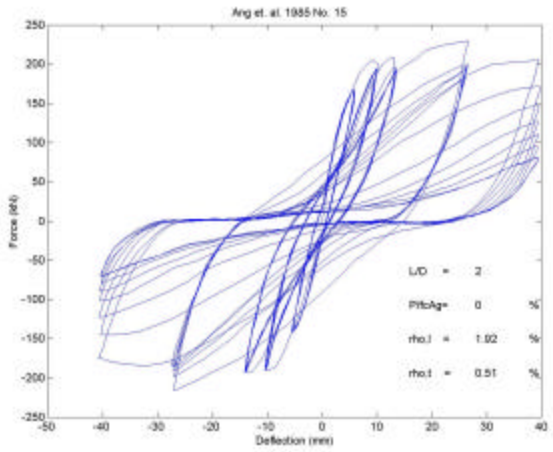
Ang et. al. 1985 No. 15
Force (kN)
Deflection (mm)
L/D = 2
P/fcAg= 0 %
rho.l = 1.02 %
rho.t = 0.51 %

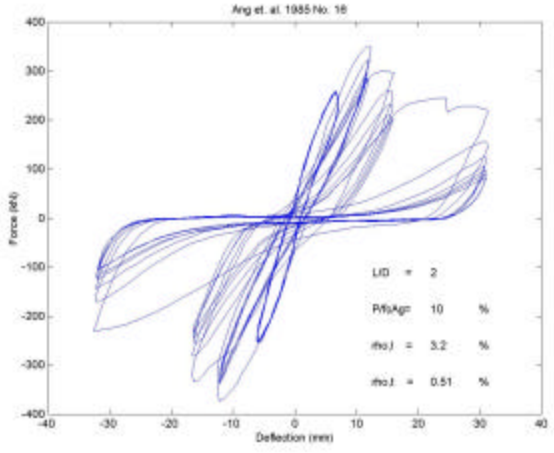
Ang et. al. 1985 No. 16
Force (kN)
Deflection (mm)
L/D = 2
P/fcAg= 10 %
rho.l = 3.2 %
rho.t = 0.51 %

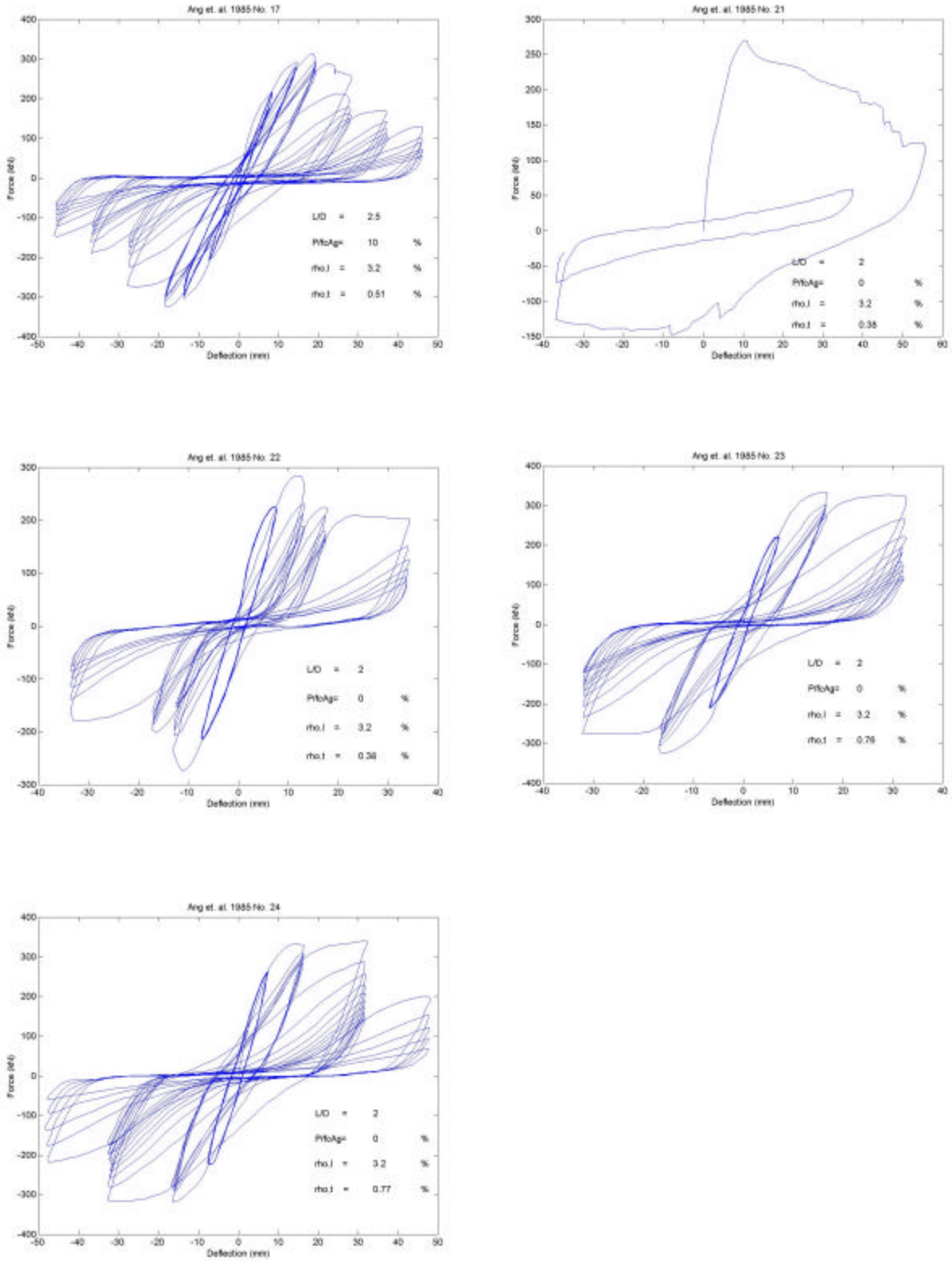

Fig. B.1 Force displacement histories (Ghee et al. 1985)

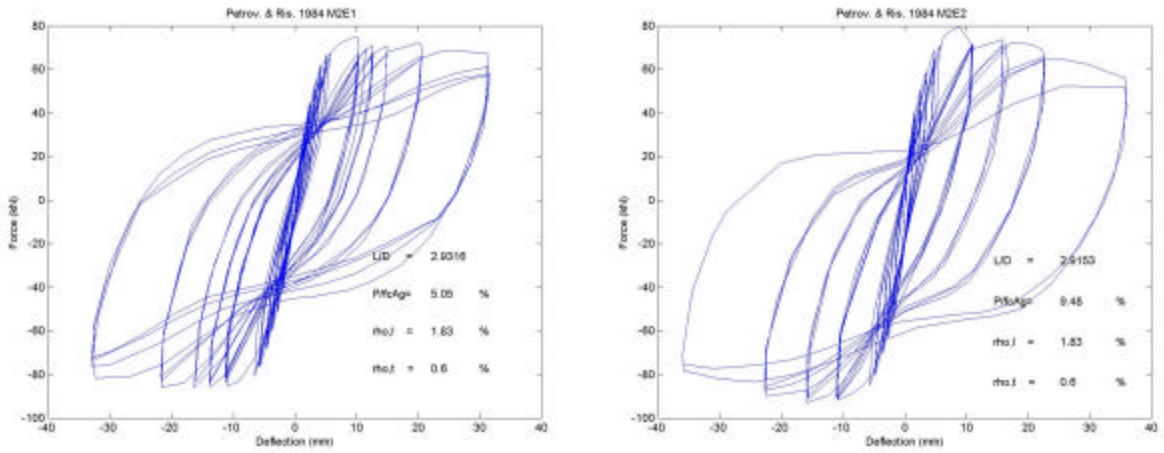

Fig. B.2 Force displacement histories (Petrovosky et al. 1984)

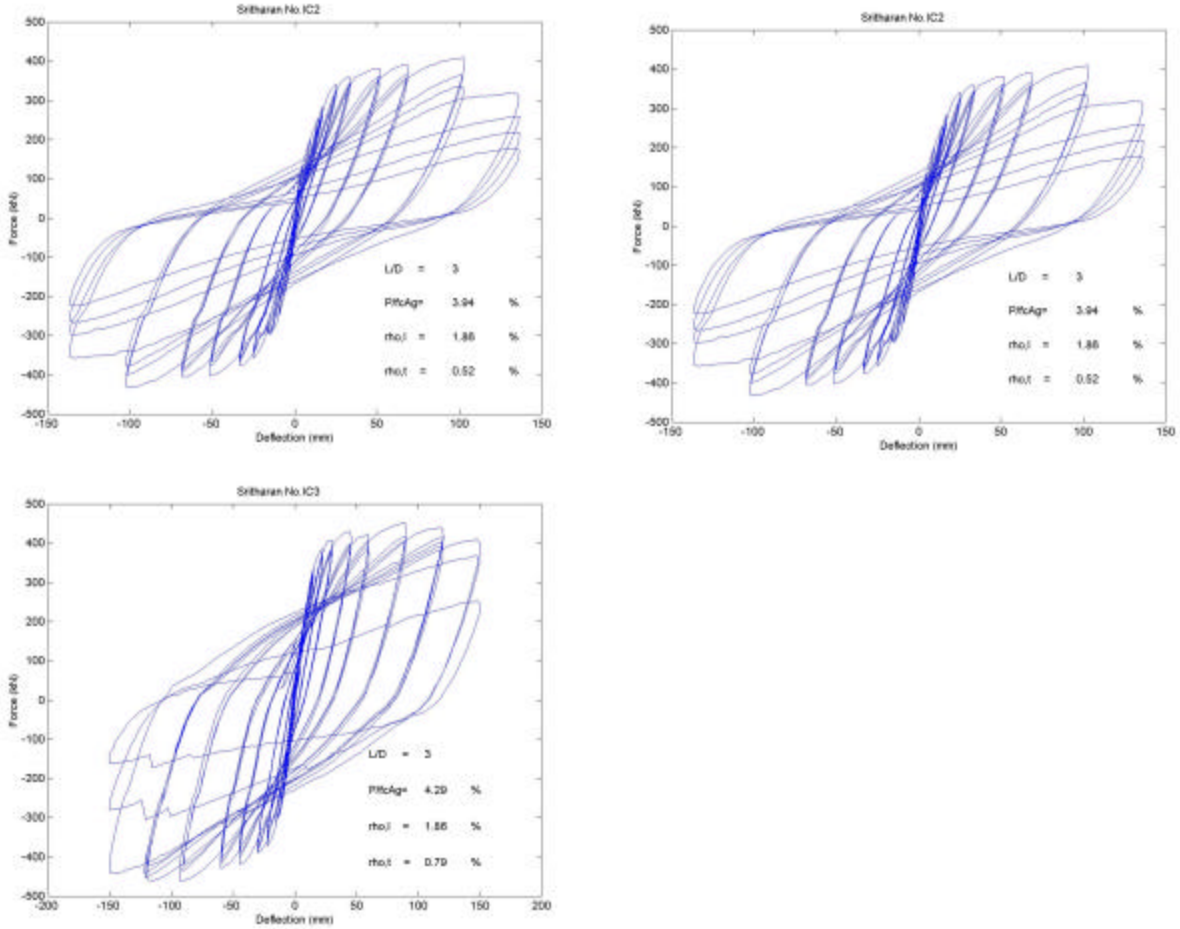

Fig. B.3 Force displacement histories (Sritharan et al. 1996)

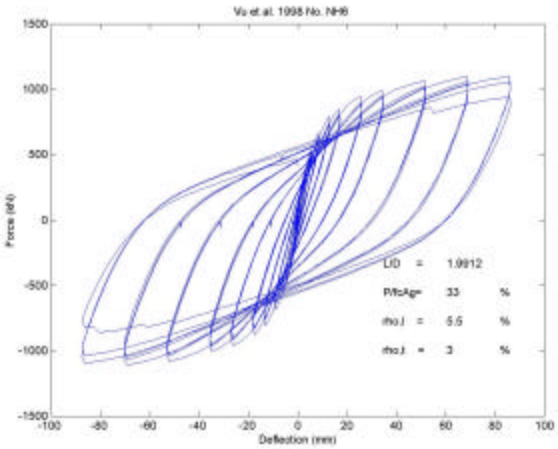

Fig. B.4 Force displacement histories (Vu et al. 1998)

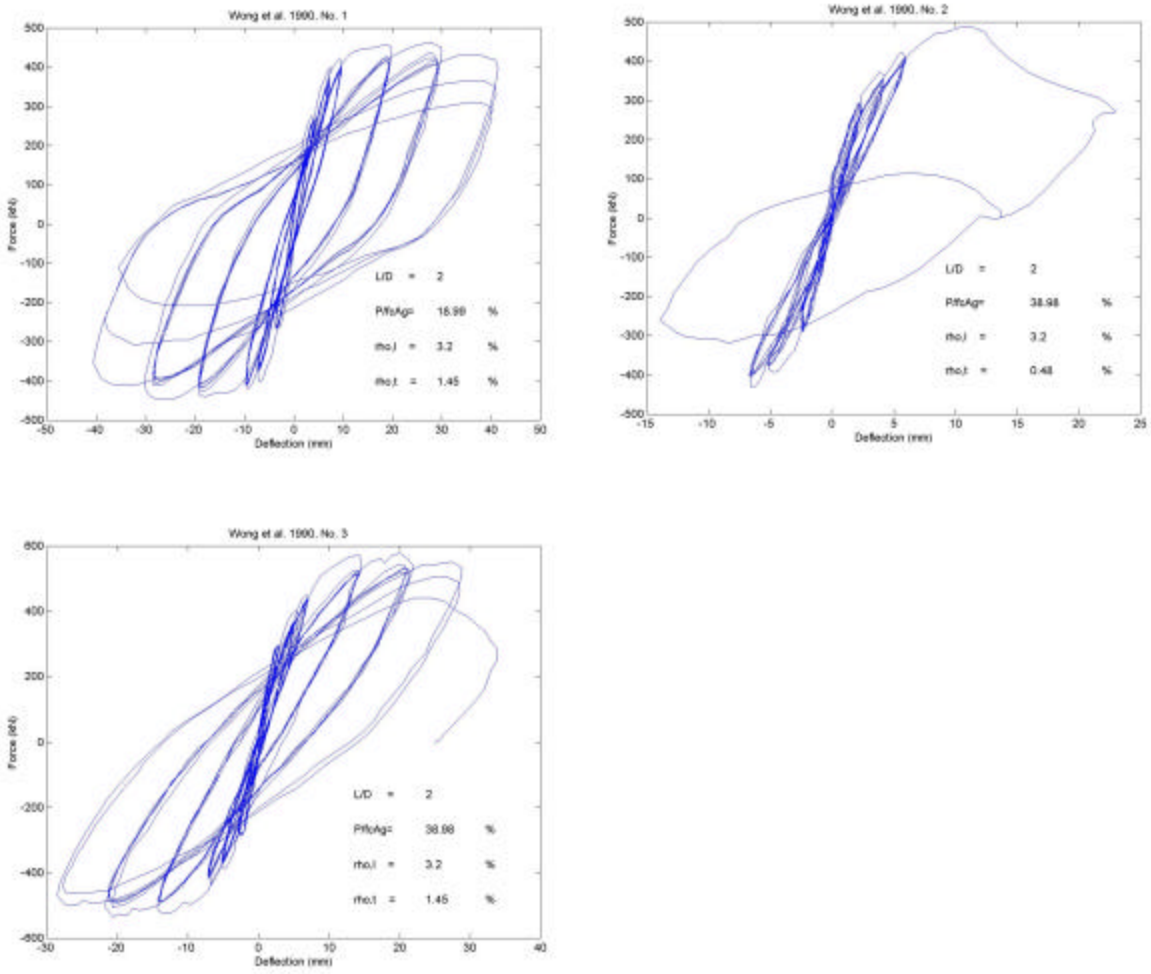

Fig. B.5 Force displacement histories (Wong et al. 1990)

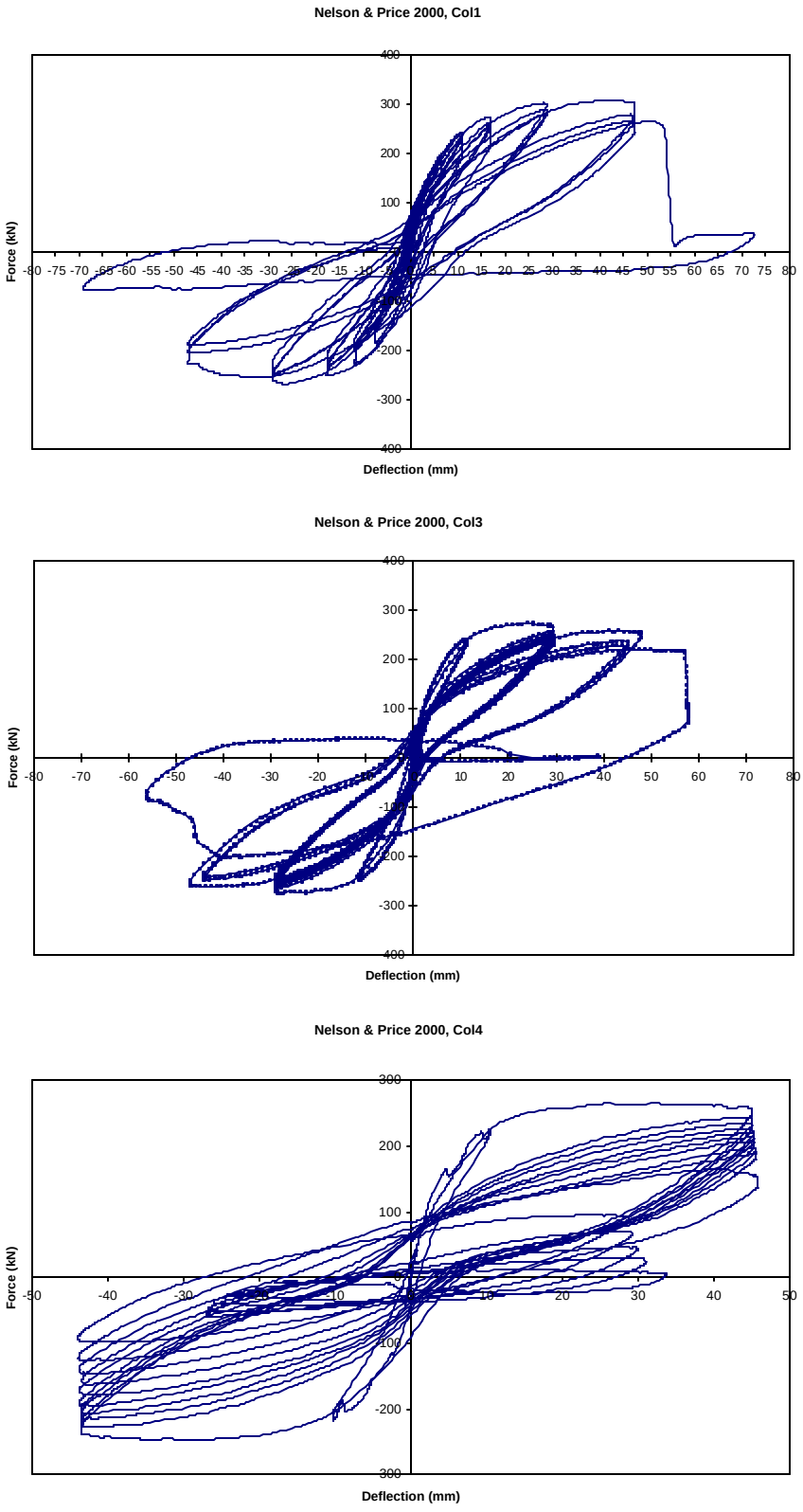

Fig. B.6 Force displacement histories (Nelson et al. 2000)

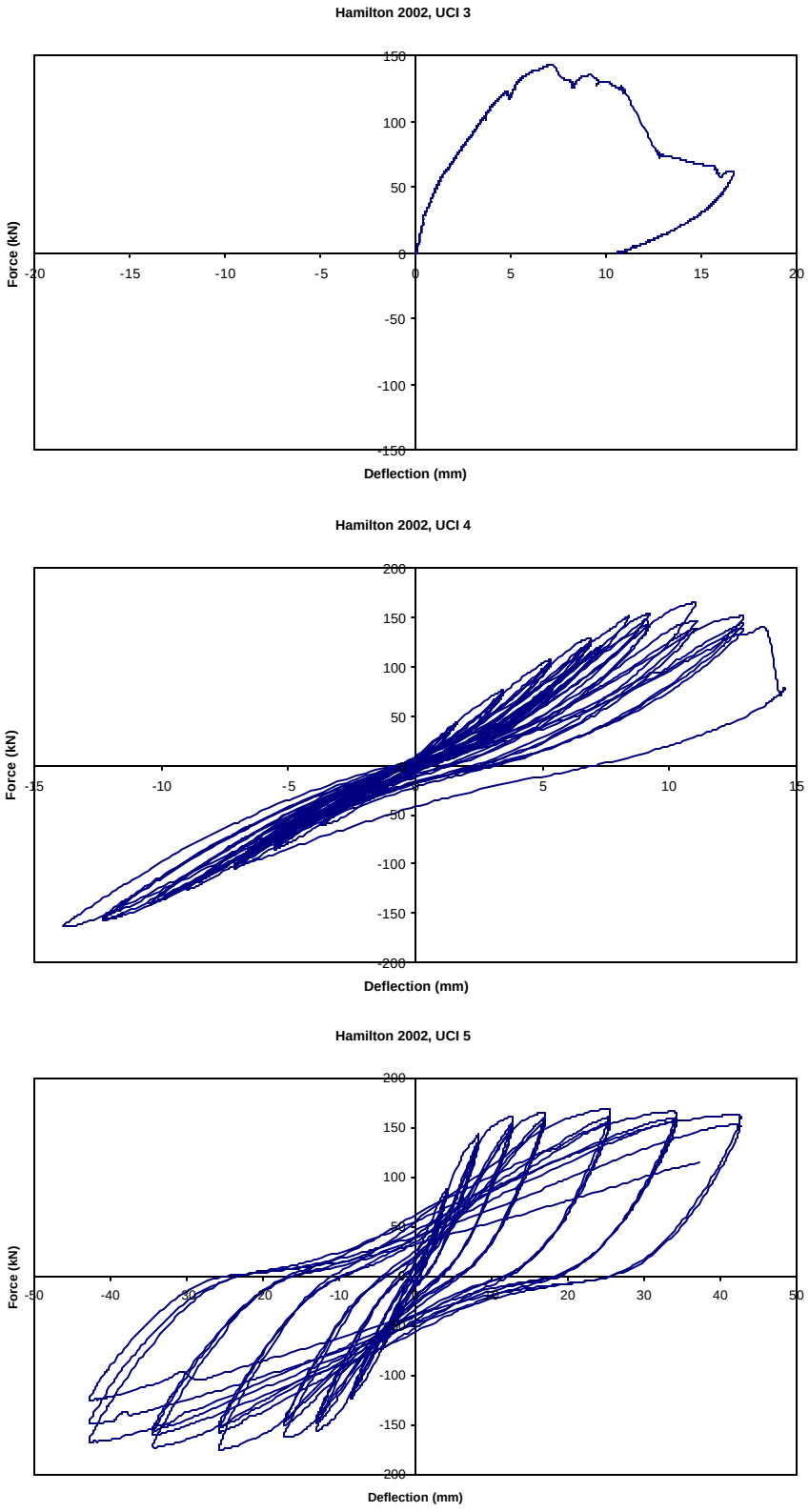

Fig. B.7 Force displacement histories (Hamilton 2002)

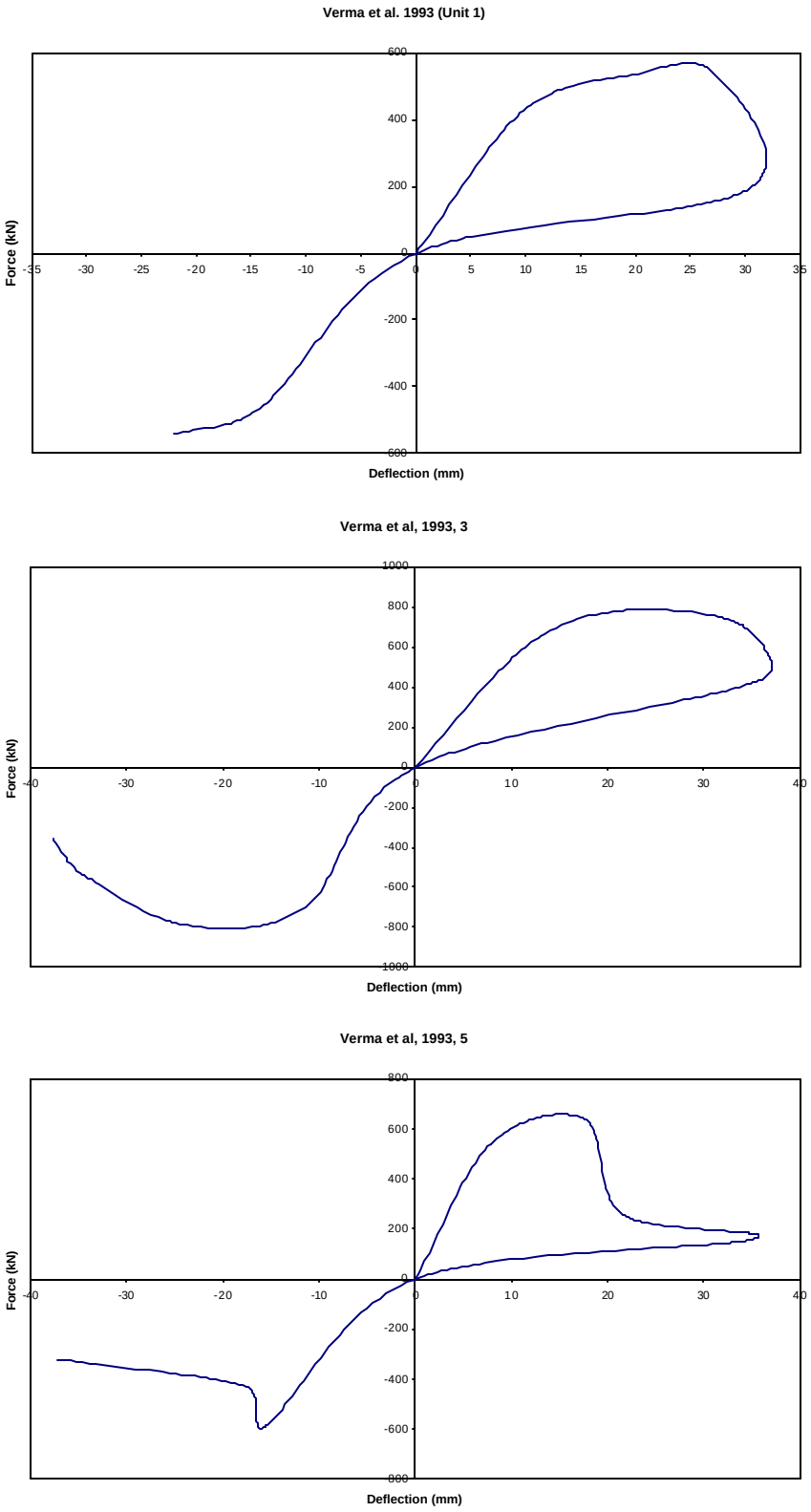

Fig. B.8 Force displacement histories (Verma et al. 1993)

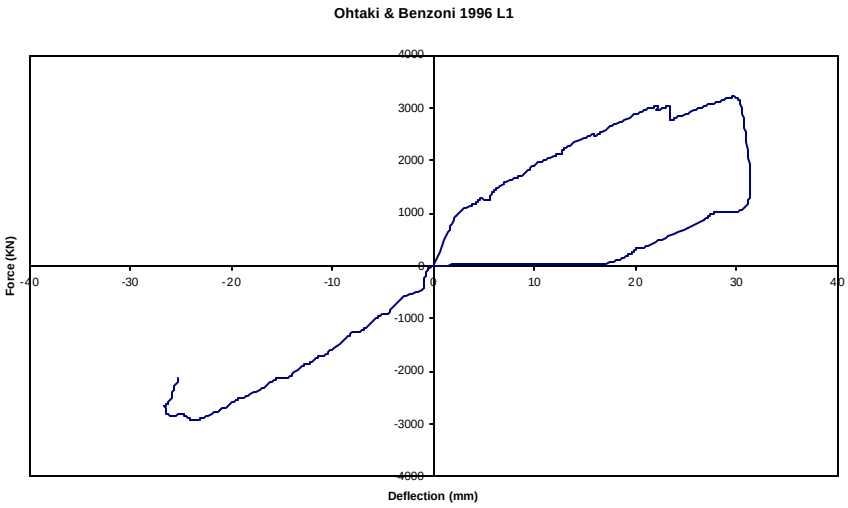

Fig. B.9 Force displacement histories (Ohtaki et al. 1997)

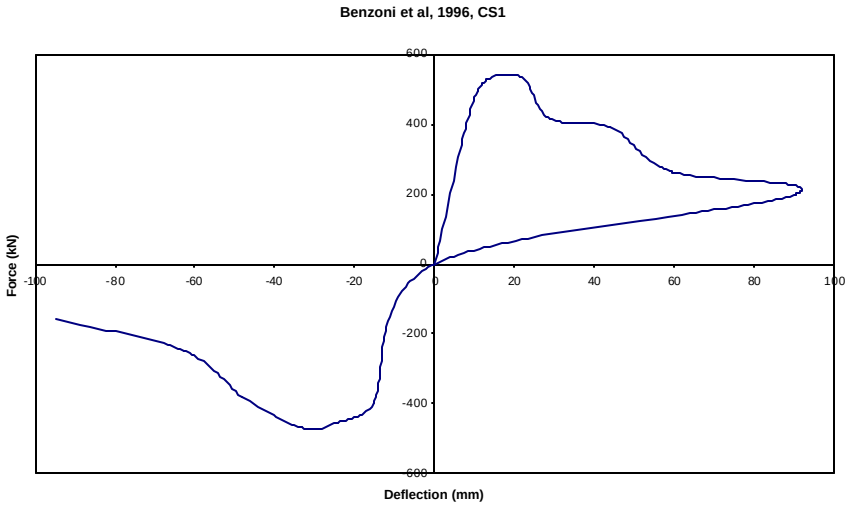

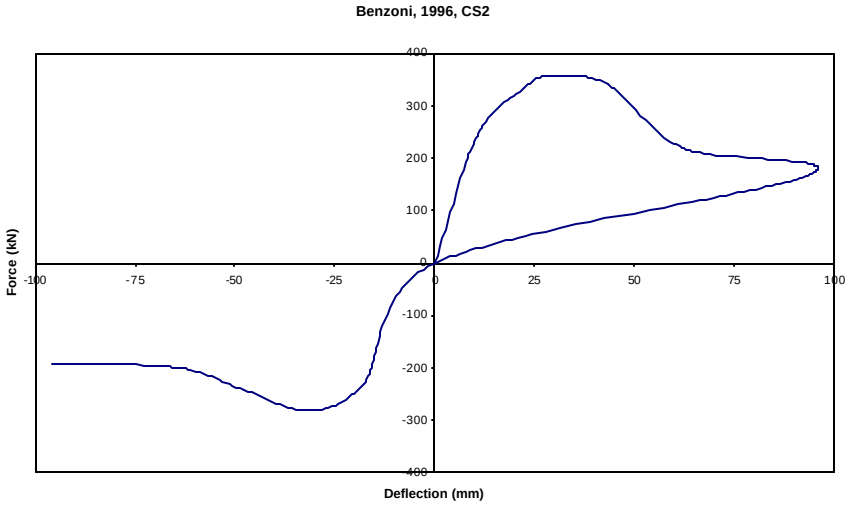

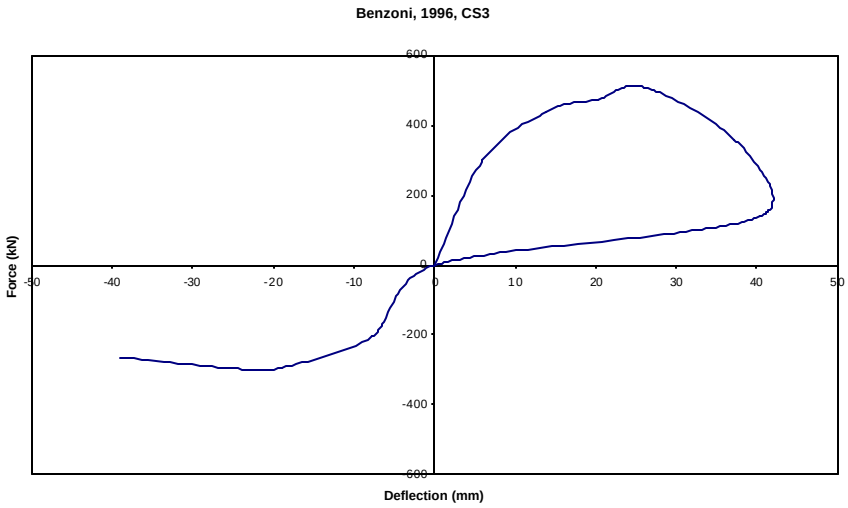

Fig. B.10 Force displacement histories (Benzoni et al. 1996)

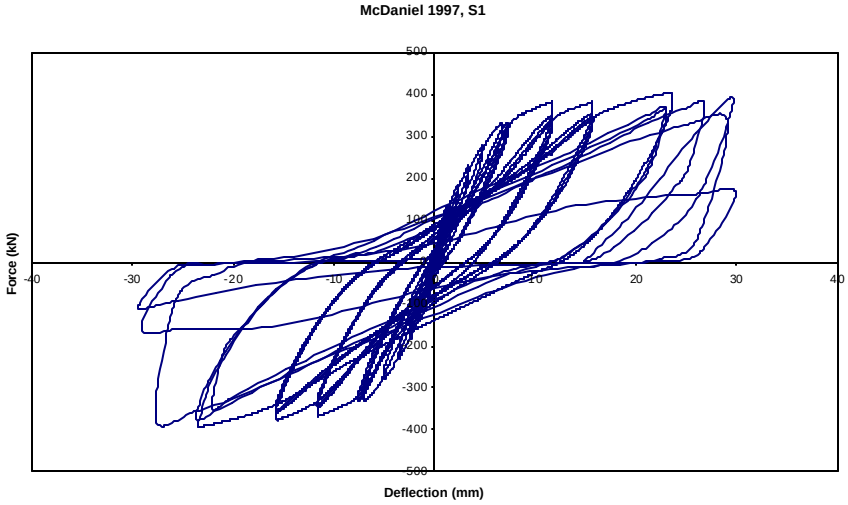

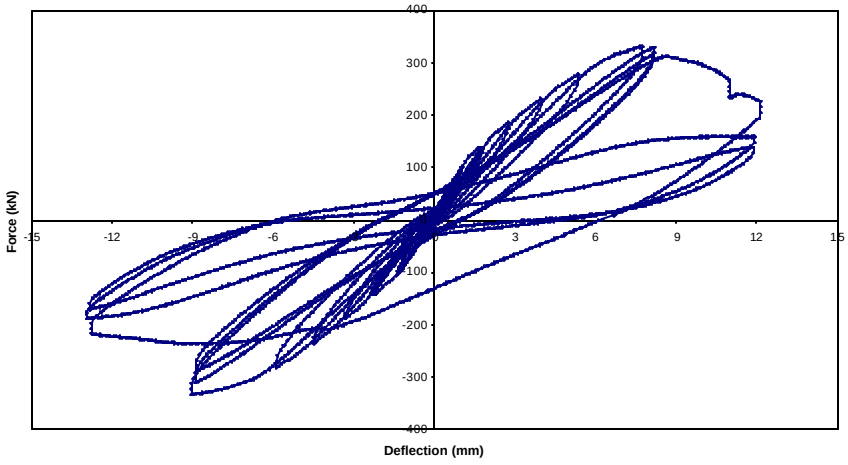

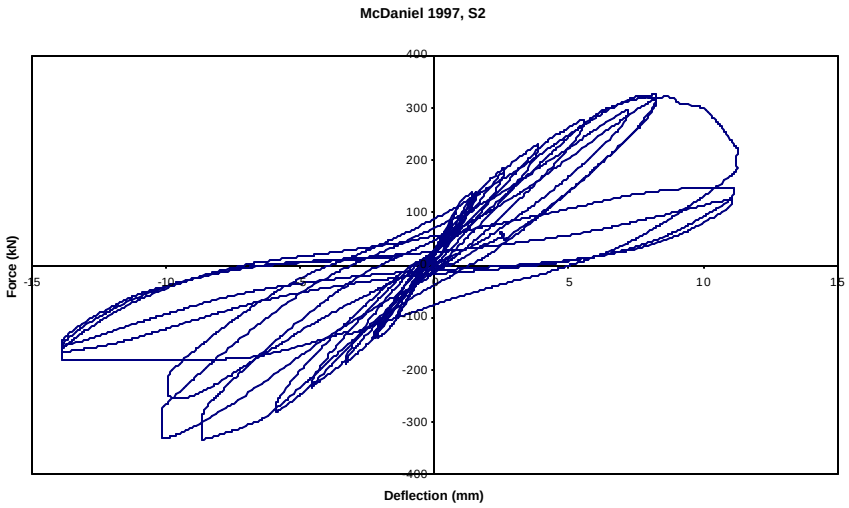

Fig. B.11 Force displacement histories (McDaniel 1997)

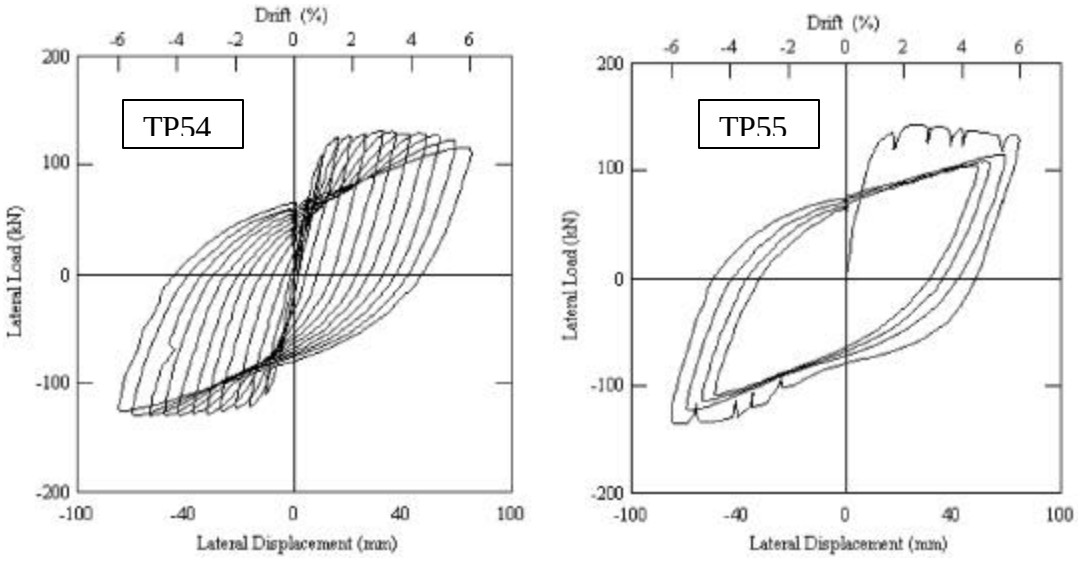

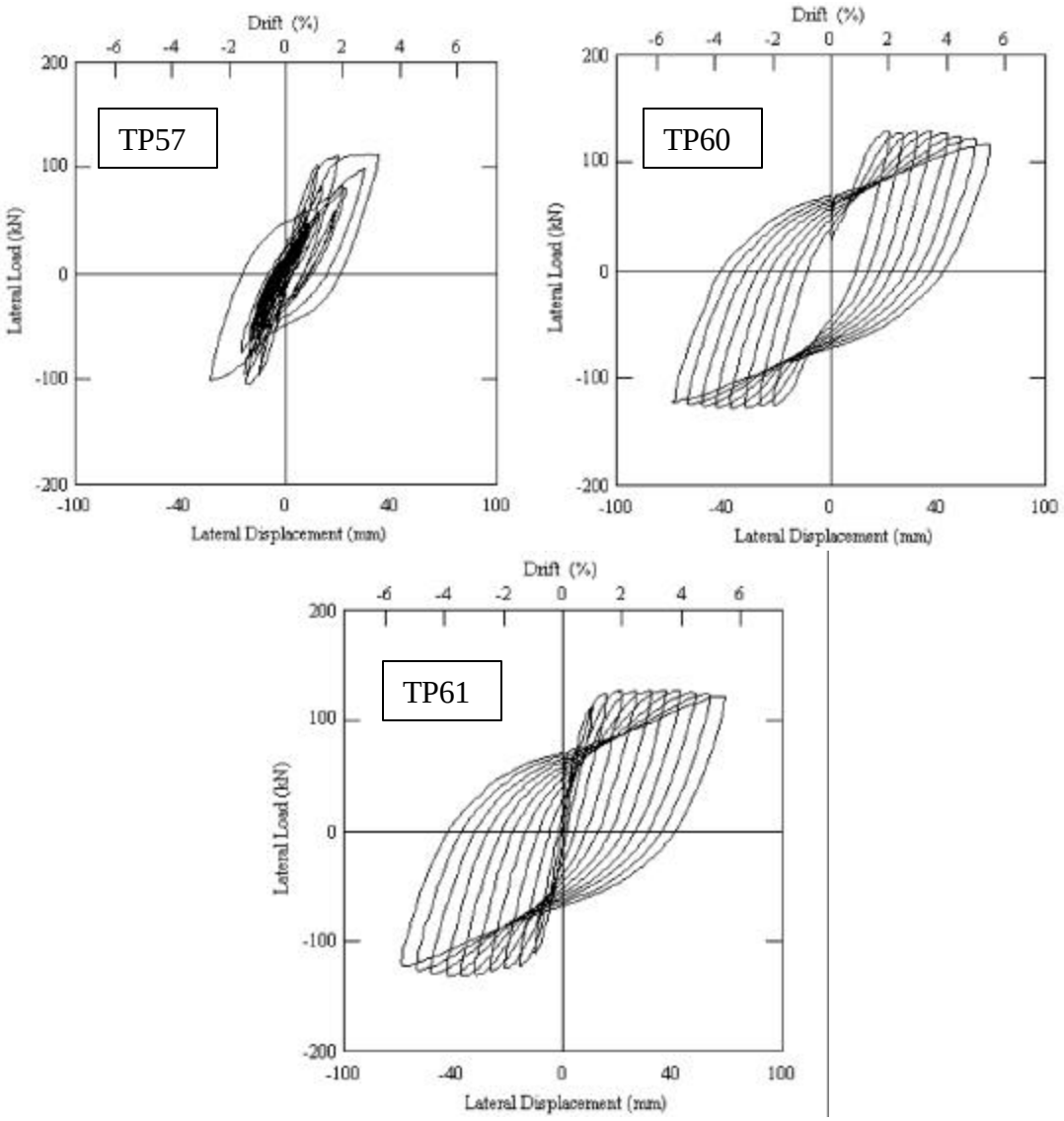

Fig. B.12 Force displacement histories (Kawashima laboratory)